From Department of Clinical Science, Intervention and Technology (CLINTEC), Division of Medical Imaging and Technology, Karolinska Institutet, Stockholm, Sweden

QUANTITATIVE EVALUATION OF LIVER FUNCTION USING GADOXETIC ACID-ENHANCED MRI

Qiang Wang

王 强

Karolinska Institutet

Stockholm 2022

Cover design “Increasing information is mining from liver specific gadoxetic acid enhanced MRI for healthcare” by the author of this book, assisted by Zhen Zheng

Published by Karolinska Institutet.
Printed by Universitetsservice US-AB, 2022

ISBN 978-91-8016-591-4

QUANTITATIVE EVALUATION OF LIVER FUNCTION USING GADOXETIC ACID-ENHANCED MRI

THESIS FOR DOCTORAL DEGREE (Ph.D.)

By

Qiang Wang

The thesis will be defended in public at Lecture Hall C1:87, Karolinska University Hospital Huddinge, Monday the 23rd of May, 2022, 13:00 pm

https://ki-se.zoom.us/j/7789583971 Meeting ID: 778 958 3971

***Principal Supervisor**:*
Professor Torkel Brismar
Karolinska Institutet
Department of Clinical Science,
Intervention and Technology (CLINTEC)
Division of Radiology

***Co-supervisor(s)**:*
Docent Ernesto Sparrelid
Karolinska Institutet
Department of Clinical Science,
Intervention and Technology (CLINTEC)
Division of Surgery

Professor Moustapha Hassan
Karolinska Institutet
Department of Laboratory Medicine
Division of Biomolecular and
Cellular Medicine (BCM)

***Opponent**:*
Associate Professor Caecilia S. Reiner
Zürich University
Institute of Diagnostic and Interventional Radiology,
University Hospital Zürich

***Examination Board**:*
Professor Lennart Blomqvist
Karolinska Institutet
Department of Molecular Medicine
and Surgery

Professor Tie-Qiang Li
Karolinska Institutet
Department of Clinical Science,
Intervention and Technology (CLINTEC)

Professor Stergios Kechagias
Linköping University
Department of Health, Medicine and
Caring Science

To my wife, and my beloved family

Three passions, simple but overwhelmingly strong, have governed my life: the longing for love, the search for knowledge, and unbearable pity for the suffering of mankind.

Bertrand Russel

ABSTRACT

Before liver resection, a reliable and accurate assessment of the liver function is essential to ensure a safe surgery and avoid unfavorable complications such as post-hepatectomy liver failure (PHLF). Gadoxetic acid enhanced magnetic resonance imaging (MRI) is a routinely used imaging modality for tumor detection and characterization. In recent years, research has shown that gadoxetic acid enhanced MRI can be a reliable and promising tool in evaluation of liver function, supplying liver function information at both global and regional levels. Accurate assessment of liver function also makes it possible to predict PHLF preoperatively.

In **Study I**, the three categories of parameters derived from gadoxetic acid enhanced MRI (signal intensity-based, T1 relaxometry-based and dynamic hepatic contrast enhanced MRI-based) were evaluated for the consistency between them and the correlation with Child-Pugh score and Model for End-stage Liver Disease score. It was shown that the simple signal intensity based parameters had a similar capacity as the complex ones in evaluation of liver function. Among them, liver-to-muscle ratio (LMR) showed a good performance and could be selected for clinical usage.

Study II was a prospective pilot study, which compared the efficacy of gadoxetic acid enhanced MRI with two gold standard tests (indocyanine green retention test at 15 min (ICG-R15) and hepatobiliary scintigraphy) in evaluation of liver function during the perioperative period. It was shown that 1) the consistency between the three modalities was good, 2) LMR and hepatic uptake index were reliable for liver function assessment and predictive for liver growth after liver resection, and 3) liver function and volume changed in parallel within one month after liver resection.

The systematic review of **Study III** was performed to summarize currently available evidence for the value of preoperative gadoxetic acid enhanced MRI in prediction of PHLF. It included 15 original studies and the results demonstrated that gadoxetic acid enhanced MRI had a high predictive value in estimation of PHLF risk, with an area under the curve ranging from 0.67 to 0.96.

In **Study IV**, a clinical model using radiomics and machine learning approaches based on hepatobiliary phase of gadoxetic acid enhanced MRI for PHLF prediction in patients with hepatocellular carcinoma was developed and validated. The prediction model yielded an AUC of 0.84 and 0.82 in the training and test cohorts respectively, showing a promising ability to stratify patients into different risk levels for PHLF.

In summary, preoperative gadoxetic acid enhanced MRI seems to be an effective and reliable imaging biomarker for quantitative evaluation of liver function and for prediction of post-hepatectomy liver failure.

LIST OF SCIENTIFIC PAPERS

I. Quantitative evaluation of liver function with gadoxetic acid enhanced MRI: Comparison among signal intensity-, T1-relaxometry-, and dynamic-hepatocyte-specific-contrast-enhanced MRI- derived parameters.
Wang Q, Kesen S, Liljeroth M, Nilsson H, Zhao Y, Sparrelid E, Brismar TB. *Scandinavian Journal of Gastroenterology*. 2022 Feb 2:1-8.

II. Multimodal perioperative assessment of liver function and volume in patients undergoing hepatectomy for colorectal liver metastasis: a comparison of the indocyanine green retention test, ^{99m}Tc mebrofenin hepatobiliary scintigraphy and gadoxetic acid enhanced MRI.
submitted manuscript

III. Predictive value of gadoxetic acid-enhanced MRI for posthepatectomy liver failure: a systematic review.
Wang Q, Wang A, Sparrelid E, Zhang J, Zhao Y, Ma K, Brismar TB.
European Radiology. 2022 Mar;32(3):1792-1803.

IV. A radiomics model based on preoperative gadoxetic acid enhanced MRI for predicting posthepatectomy liver failure in patients with hepatocellular carcinoma.
submitted manuscript

CONTENTS

LIST OF ABBREVIATIONS

ΔLMR	Increase rate of LMR
ΔR1	Increase in the relaxation rate
ALBI	Albumin-bilirubin score
ALT	Alanine aminotransferase
AST	Aspartate transaminase
AUC	Area under the receiver operating characteristic curve
CI	Confidence interval
CLD	Chronic liver disease
CRLM	Colorectal liver metastases
DCA	Decision curve analysis
DHCE-MRI	Dynamic hepatocyte-specific contrast enhanced MRI
FLR	Future liver remnant
FLR-F	Future liver remnant function
FLR-V	Future liver remnant volume
HEF	Hepatic extraction fraction
HBP	Hepatobiliary phase
HBS	Hepatobiliary scintigraphy
HUI	Hepatocellular uptake index
ICC	Intraclass coefficient
ICG-R15	Indocyanine green retention test at 15 min
INR	International normalized ratio
ISGLS	International Study Group of Liver Surgery
increFLR_F	FLR increase rate in function
increFLR_V	FLR increase rate in volume
irBF	Input-relative blood flow

KGR-F	Kinetic growth rate in function
KGR-V	Kinetic growth rate in volume
K_{hep}	Hepatic uptake rate
LASSO	Least absolute shrinkage and selection operator
LMR	Liver-to-muscle ratio
LSC_N20	Liver-spleen contrast ratio at 20min after contrast agent injection
LSR	Liver-to-spleen ratio
MELD	Model for End-Stage Liver Disease
MTT	Mean transit time
OATP	Organic anion transporter polypeptide
PHLF	Post-hepatectomy liver failure
POD	Postoperative day
PVE	Portal vein embolization
pVol	Liver parenchymal volume
QUIPS	Quality In Prognostic Studies tool
RLE	Relative liver enhancement
ROI	Region of interest
SI	Signal intensity
SPECT	Single-photon emission computed tomography
sFLR-F	Standardized FLR-F
sFLR-V	Standardized FLR volume
$T1_{20min}$	T1 relaxation time at 20 min after contrast agent injection
T1red	Reduction rate of T1 relaxation time
tVol	Total liver volume

1 INTRODUCTION

Cancer occurring in the liver includes primary liver cancer and secondary liver cancer (metastasizing from other organs) (1). Hepatocellular carcinoma (HCC) is the most common type of primary liver cancer and ranks the sixth in prevalence of new cancer cases and the third leading cause for cancer-related death worldwide, with an estimation of 782,000 new cases and 746,000 deaths every year, respectively (2). The risk factors of HCC include chronic liver disease (mainly infected by hepatitis virus B or C), exposure to aflatoxin B1 in diet and alcohol abuse (3-5). Liver fibrosis/cirrhosis of any cause significantly increases the risk of HCC incidence. With the obesity and metabolic syndrome becoming a common issue in developed regions, non-alcoholic fatty liver disease has jumped to a main cause of the increasing incidence of HCC (2). Due to its latent feature, most HCCs have developed into an advanced stage with a large tumor size when first diagnosed (6). Regarding secondary liver cancer, it is most often caused by metastases from colorectal cancer. This is explained by its high incidence, being the second most frequent cancer worldwide combined with a high metastasizing frequency (7). Approximately 40-50% of the colorectal cancer patients develop liver metastases at either diagnose (synchronous metastasis) or later (metachronous metastasis) (8). Colorectal liver metastases (CRLM) often present as multifocal lesions spread among right and/or left hemiliver.

Liver resection remains the mainstay treatment for liver cancer with a potential benefit for the long-term outcome (9, 10). During the past decades, with the advance of surgical devices, perioperative management, and anesthetic techniques, the resectability rate of liver cancer is increasing (11, 12). Nevertheless, extended liver resection is mainly limited by the insufficient future liver remnant (FLR) given the above-mentioned facts that HCC is often diagnosed at an advanced stage with large tumor size and CRLM with multifocal lesions (8, 13).

Regarding the FLR, many strategies have been proposed to induce FLR hypertrophy during the last decades to increase the number of candidate patients for liver resection, including portal vein embolization/ligation (14-16) and two-stage hepatectomy, such as associating liver partition and portal vein ligation for staged hepatectomy (17-19). On the other hand, reliable evaluation of the FLR function is of clinical importance to avoid the lethal complications, for instance post-hepatectomy liver failure (PHLF) (20, 21), considering that patients with liver malignance are often accompanying with liver function impairment and the distribution of liver function is unevenly.

2 BACKGROUND

Until now, several modalities have been applied for liver function evaluation before liver resection.

2.1 MODALITIES FOR EVALUATION OF LIVER FUNCTION

2.1.1 Serum biochemical test

Serum biochemical tests are simple, fast, and highly accessible methods for liver function evaluation. They are commonly used in clinical practice including aspartate aminotransferase (AST), alanine aminotransferase, bilirubin, albumin and prothrombin time. However, these parameters just provide a big picture of the liver function: some of them are not specific for the liver (for instance AST) (22) and some parameters cannot "real time" monitor the liver function changes (e.g. albumin) (23). Besides, all of these parameters just evaluate the liver function as a whole, which cannot satisfy the surgeons' clinical need for local liver function assessment.

The serum biochemical tests can be integrated to form a compound index to better evaluate liver function. One representative index is the albumin-bilirubin (ALBI) grade (24). It is calculated by the formula: ALBI score = (log10 bilirubin × 0.66) (albumin × 0.085). The obtained score is further categorized into Grade 1 (≤ -2.60), Grade 2 (more than -2.60 to ≤ -1.39) and Grade 3 (> -1.39), representing a decreasing liver function (24). ALBI grade has proven to be an objective and reliable parameter for liver function evaluation and it has been validated across several geographical regions (25).

2.1.2 Clinical scoring system

Child-Pugh score and Model for End-stage Liver Disease (MELD) are two widely used scoring systems for evaluation of the severity of chronic liver disease (23). They have been adopted in several guidelines for treatment recommendation (26). The Child-Pugh scoring system employs five measurements, including albumin, bilirubin, prothrombin/international normalization ratio (INR), ascites and hepatic encephalopathy. It assigns patients into Class A, B and C with decreasing liver function (27, 28). The MELD score is determined by three serum biochemical tests via the formula: 3. 8×ln [serum bilirubin] + 11.2×ln [INR] + 9.6×ln [serum creatinine] + 6.4(29). However, neither of the two scoring systems is able to estimate the risk of PHLF (23, 30).

2.1.3 Indocyanine green test

Indocyanine green (ICG) is a non-toxic, inert water-soluble dye. After administration, it is mainly bound to lipoproteins and is exclusively absorbed by hepatocytes. It is excreted into the bile and feces without biotransformation nor enterohepatic re-circulation (31). Its elimination rate is used to reflect liver function. The retention test at 15 minutes after injection (ICG-R15) is most often applied for quantitative assessment of liver function.

ICG test is often regarded as the gold standard for quantitative evaluation of liver function before liver resection, especially in East Asian countries (32, 33). However, the ICG test can be influenced by several factors, such as the hepatic blood flow, hyperbilirubinemia, use of vasodilator or any disorder affecting bile excretion (31, 34, 35). The results should be interpreted with caution when ICG test is applied in those situations. Another drawback of the ICG test is that it only supplies liver function information of the whole liver.

2.1.4 Hepatobiliary scintigraphy examination

Hepatobiliary scintigraphy (HBS) examination with ^{99m}Tc-mebrofenin is a nuclear medicine approach for global and regional liver function evaluation (23). After injection intravenously, dynamic scintigraphy is conducted by using a gamma camera. From the obtained images, the uptake rate of ^{99m}Tc-mebrofenin is determined by delineating a ROI around the liver and the FLR(36). HBS still serves as a gold standard for local liver function evaluation. Nevertheless, the wide utility of HBS is hampered by its low spatial resolution and radiation exposure. Besides, the device is not accessible at all levels of medical centers.

2.1.5 Liver volumetry

Presently, liver volumetry is mainly achieved by computed tomography (CT) due to its wide accessibility, fast scanning speed and low cost, which serves as a proxy for quantitative liver function assessment. The commonly accepted volume limit after hepatectomy is >25-30% for normal liver tissue, and >40% for damaged liver, for instance liver cirrhosis or cholestasis (37). Insufficient liver function after hepatectomy would result in post-hepatectomy liver failure, a lethal complication. CT-based liver volumetry is still one of the key references when planning liver resection in current clinical practice. However, this approach is based on the basic assumption that the liver function is distributed evenly across different liver segments.

However, this assumption is contradictionary to the fact that most liver cancers are accompanied with chronic liver disease or post-chemotherapy and these chronic processes have already lead to heterogeneous distribution of liver function (34, 38).

2.2 GADOXETIC ACID ENHANCED MRI

2.2.1 Basic characteristics

Gadoxetic acid (Gd-EOB-DTPA, Primovist®) is a paramagnetic contrast medium which increases the tissue T1 relaxivity. Normal hepatic parenchyma will thereby be enhanced and appear with higher signal (whiter) on T1-weighted images (39). The special property of gadoxetic acid is that about 50% is absorbed by the hepatocytes after injection, in comparison to the 5% for the other available liver-specific contrast medium Gd-BOPTA (gadobenate disodium) (40). The optimal enhancement effect occurs between 10-40 min after injection, the so-called hepatobiliary phase (40, 41). In clinical practice, imaging 20 minutes after injection is most often used for analysis (42).

When administered into the blood, gadoxetic acid is transported by two hepatocyte transport systems: uptake by the transporting polypeptides (Organic anion transporter polypeptides, OATPs, including OATP1B1 and 1B3) on the sinusoidal membrane and excretion by multidrug resistance-associated proteins (MRPs, MRP2) on the canalicular membrane, without undergoing biotranformation (40, 41, 43). With the progress of liver disease, the activity of OATPs is decreased, while MRPs activity is increased. This results in a net decreased enhancement of the liver parenchyma (40). A plenty of studies have shown this inverse correlation between liver disease and liver enhancement (34, 44). It is of note to point out that also the ICG test and hepatobiliary scintigraphy evaluate liver function based on the expression of OATP1B1/1B3 transporter (23, 40, 41).

2.2.2 Three categories of parameters

There are three main approaches to quantify liver function based on the enhancement of liver parenchyma by MRI: direct measurement of signal intensity (SI), T1 relaxometry (i.e. measurement of the T1 relaxation time) and dynamic hepatic contrast-enhanced MRI (DHCE-MRI) (22, 41, 45).

SI-related parameters are the most commonly used, as they are easy-to-get and can be obtained through common scanning sequences. However, they describe a relative index on an arbitrary

scale, making comparisons among patients impossible (46). SI-related parameters can also be influenced by many technical factors such as the MRI scanner strength, MR coil, pulse sequence and technical parameters used (41, 46).

T1 relaxometry reflects the intrinsic characteristic of the liver tissue, which is more stable, not affected by pulse sequence or exact imaging parameters. Its widespread usage, however, is hindered by the requirement of additional imaging sequences compared to standard clinical imaging and its rather complex calculation (45, 47, 48).

DHCE-MRI evaluates liver function by measuring a time-intensity curve of hepatic parenchyma and vessels based on complex pharmacokinetic modelling. It can supply additional hepatic perfusion information from clinical images and takes the whole liver into account, but it involves complicated calculations (34, 49-51) (Table 1).

Table 1. Gadoxetic acid enhanced MRI derived parameters for liver function assessment

	Representative parameters	**Simplicity**	**Key confounder**	**Additional imaging sequence required**
Signal intensity measurement	RLE, LMR, LSR & HUI	+++	Technical factors, such as scanner, coil	-
T1 relaxometry	T1 relaxation time, K_{hep}	++	Hepatic blood flow	+
DHCE-MRI	HEF, MTT & irBF	+	Hepatic hemodynamic process and complex data analysis	+

Note: DHCE-MRI, dynamic hepatic contrast enhanced MRI; HEF, hepatic extraction fraction; HUI, hepatocellular uptake index, irBF, input-relative blood flow; K_{hep}, hepatic uptake rate; LMR, liver-to-muscle ratio; LSR, liver-to-spleen ratio; MTT, mean transit time; RLE, relative liver enhancement.

2.2.3 Radiomics

Radiomics is a burgeoning approach which, taking advantage of computer techniques, can extract high throughput imaging features from clinically routinely-used images and convert them into minable data (52, 53). Through machine learning algorithms, a prediction model for diagnosis or prognosis can be constructed. The basic assumption underlying the radiomics

approach is that the subtle alterations at the genetic/molecular level can be manifested in the imaging texture (54, 55). By detecting and quantifying these changes, radiomics have shown an encouraging potential in screening, diagnosis, grading and prediction of treatment in cancers (56, 57).

In recent years, studies have also investigated the radiomics methods in evaluation of liver function and in prediction of PHLF (58-63). However, these studies were exploratory and limited by small sample size or lacking external validation. Before translating into clinical utility, the reproducibility and reliability of the model should be well addressed.

2.3 POST-HEPATECTOMY LIVER FAILURE

2.3.1 Incidence and definition

One of the lethal complications after liver resection is post-hepatectomy liver failure (64-66), with incidence ranging from 4 to 40% according to different criteria applied and the experience of the individual medical center (67, 68). Once occurring, a mortality as high as 80% has been reported (69, 70).

Many a researcher have proposed a definition for PHLF. The most commonly used definition is the one made by the International Study Group of Liver Surgery (ISGLS). This is due to its simplicity and operability. It defines PHLF as when an increased INR and hyperbilirubinemia is present on postoperative day 5 or afterwards (71). According to the clinical intervention involved, PHLF is further divided into Grade A (no change is required about the patient postoperative management), Grade B (the patient management deviates from the regular course but no invasive treatment is needed) and Grade C (invasive treatment is required) (71). Another commonly used definition of PHLF is the "50-50 criteria", in which on postoperative day 5, there is both prothrombin time < 50% and bilirubin > 50 μmol/L (72).

2.3.2 Risk factors and predictors for PHLF

Many clinical factors exert an effect on the probability of PHLF and they can loosely be grouped into patient-related, liver-related, and surgery-related risk factors (32, 33, 73) (Table 2).

Table 2. Clinical risk factors for post-hepatectomy liver failure

Patient related	Liver related	Surgery related
Male	Chronic liver disease	Extended resection
Age ≥ 65 years	Hepatitis	Intraoperative blood loss > 1000 ml
Body Mass Index ≥ 30 kg/m^2	Fibrosis/cirrhosis	Intraoperative hypotension
Diabetes mellitus	Steatosis	Vascular reconstruction
Sepsis	Cholestasis	Prolonged Pringle maneuver
Malnutrition	Portal hypertension	Postoperative hemorrhage
Thrombocytopenia	Chemotherapy-related liver injury	

2.3.3 Treatment and management of PHLF

Until now there is no effective treatment at PHLF but supportive care (73). It includes blood transfusion, infusion of albumin, plasma, fibrinogen and nutrient supplementation to support the failing systems (73, 74). Molecular adsorbent recirculating system, an albumin-based system, was shown a safe and feasible treatment to support patients for spontaneous recovery or as a bridge for liver transplantation (75, 76). Liver transplantation leaves the only hope when all these supportive therapies fail (73, 77). Prevention is therefore of great importance to avoid this life-threatening condition. A body of studies have attempted to apply preoperative indicators to identify the patients with the highest risk of PHLF (68).

3 RESEARCH AIMS

The aims of this thesis were:

Aim I: To compare the efficiency of the three categories of parameters derived from gadoxetic acid enhanced MRI in quantitative assessment of liver function.

Aim II: To evaluate the dynamic changes of liver function and volume of the future liver remnant in perioperative period, and to evaluate the value of preoperative liver function in prediction liver growth after hepatectomy.

Aim III: To systematically review the efficacy of gadoxetic acid enhanced MRI derived parameters in prediction of PHLF.

Aim IV: To develop and validate a radiomics model based on preoperative gadoxetic acid enhanced MRI and clinicopathological variables for predicting PHLF in patients with HCC.

4 MATERIALS AND METHODS

4.1 Overview of the four studies

Table 3. Summary of the four studies included in this thesis

	Study I	Study II	Study III	Study IV
Study design	Retrospective	Prospective	Systematic review	Retrospective
Study period	2005.01-2007.08; 2010.02-2010.11	2014.11-2019.03	2011.08-2020.09	2017.01 – 2019.03
Data source	Single center (Karolinska University Hospital, Sweden)	Single center (Karolinska University Hospital, Sweden)	15 studies from four public databases	Single center (Southwest Hospital, China)
Participants	Health volunteers; Patients with chronic liver disease	Patients with CRLM undergoing hepatectomy	Patients undergoing hepatectomy	Patients with HCC undergoing hepatectomy
Sample size	30 (20 + 10)	10	1327	276
Liver function modality	Gadoxetic acid enhanced MRI, laboratory tests	Gadoxetic acid enhanced MRI, ICG-R15 &HBS	Gadoxetic acid enhanced MRI &ICG test	Gadoxetic acid enhanced MRI, ICG-R15, laboratory tests
MRI parameter category	SI, T1 relaxometry& DHCE-MRI	SI	SI, DHCE-MRI& Radiomics	Radiomics features
Gold standard	Child-Pugh score, MELD score	ICG-R15, HBS	ISGLS criteria for PHLF	ISGLS criteria for PHLF
Primary outcome	Consistency of three categories of MRI parameters	Consistency between liver volume and function; correlation between MRI and ICG-R15/HBS	AUC of MRI parameters for PHLF prediction	Radiomics model for PHLF prediction
Secondary outcome	Correlation between MRI parameters and Child-Pugh/MELD score	MRI parameters for liver growth prediction	ICG test vs MRI parameters for PHLF prediction	Clinical risk factors for PHLF
Main statistical methods	Mann-Whitney U test, Spearman correlation analysis	Mann-Whitney U test, Spearman correlation analysis, repeated measures analysis of variance, linear regression analysis	N.A	Uni-/multivariable regression analysis, Intraclass correlation analysis, LASSO.
Study highlight	Three categories of MRI parameters	Three modalities at three time points	Pooling analysis of current evidence	Machine learning

4.2 Study I & II

Study Design and Patients

In **Study I** 10 patients aged between 18 and 65 years old with chronic liver disease and neither hepatic surgery history nor renal dysfunction were included. Another 20 healthy volunteers were included as a control group. Subjects' demographic information, laboratory tests and gadoxetic acid enhanced MRI data were collected.

Study II was a single center, prospective study where patients with CRLM subject to right hemihepetectomy between April 2016 and July 2019 at Karolinska University Hospital, Stockholm, Sweden were initially enrolled. Patients aged less than 18 years old or with any manipulations on the FLR (such as radiofrequency ablation or tumor enucleation) were not eligible for this study. On the day before operation, on postoperative day (POD) 7 and on POD 28, all patients underwent liver function evaluation using three different techniques; ICG-R15, HBS and gadoxetic acid enhanced MRI. The timeline of these three modalities is illustrated in Figure 1.

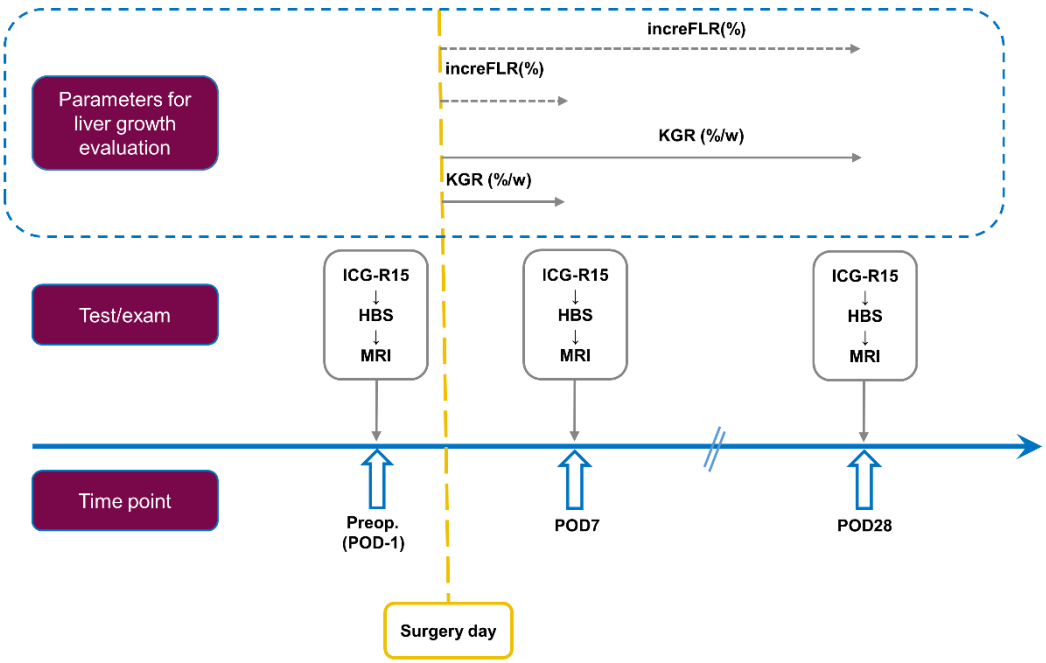

Figure 1. Timeline of the three modalities for liver function evaluation at three time points during the perioperative period. *To avoid the potential interaction, on the exam day, the ICG-R15 test was carried out first, one hour later, the HBS exam was performed, followed by the MRI with 7-8 hours apart. Note: ICG-R15, indocyanine green retention test at 15 min; increFLR, increase rate of the future liver remnant; HBS, hepatobiliary scintigraphy; KGR, kinetic growth rate; POD, postoperative day.*

Gadoxetic acid enhanced MRI acquisition

All patients in **Study I** and **II** underwent MRI examination on a 1.5 T scanner (Intera; Philips Medical Systems, Best, the Netherlands) using the same scanning protocol. Pre- and dynamic contrast enhanced images were obtained using a T1 weighted three-dimensional spoiled gradient-echo sequence. The scanning parameters were: repetition time/ echo time: 4.1/2.0 ms; flip angle: 10°; field of view: 415 mm; reconstruction matrix: 256 × 256. A total of 40 slices with slice thickness of 10 mm and overlap of 5 mm were collected. Gadoxetic acid (Primovist ®, Bayer Pharma, Germany) was injected in a standard way: at a dosage of 0.1 mL/kg body weight (concentration: 0.25 mmol/mL) through the anterior cubital vein at an injection rate of 2 mL/s, followed by an immediate flush of 20 mL saline. Images of the hepatobiliary phase (HBP) were obtained 20 min after contrast media administration.

Imaging analysis and calculation of liver function parameter

Cross-sectional images before contrast media injection (Pre) and during the HBP were exploited to calculate the liver function parameters. In brief, one slice at the level of the portal vein bifurcation was selected and several regions of interest (ROIs) were placed to measure the signal intensity (SI) values. The ROIs placements were: three in the liver (left lobe, segment IV and right lobe), one in the spinal erector muscle and one in the spleen (Figure 2). At post-hemihepatectomy (**Study II**), only two ROIs were placed in the liver (left lobe and segment IV). An average of the ROIs in the liver was assigned for the liver.

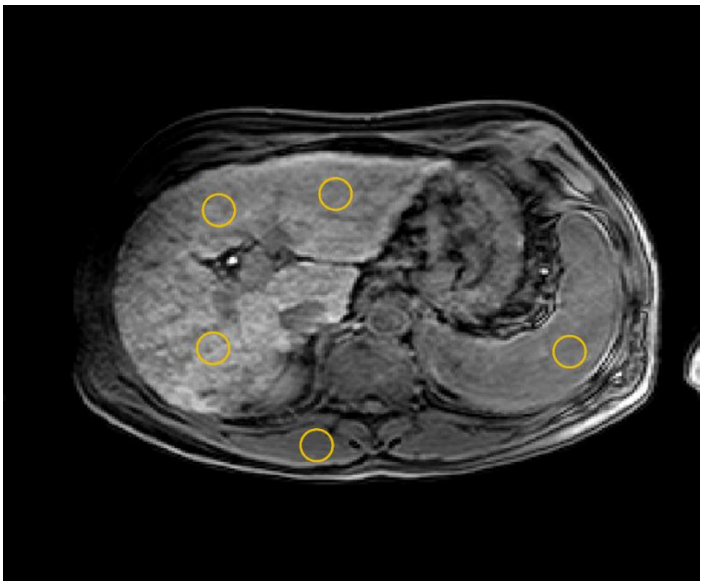

Figure 2. Measurement of the signal intensity value in the liver, muscle and spleen during hepatobiliary phase.

The formulas of the parameters used in this study were:

1. Relative liver enhancement (RLE) (46, 78, 79):

RLE = (SI_{20min} of the liver – SI_{pre} of the liver) / SI_{pre} of the liver

2. Liver-to-spleen ratio (LSR) (80):

LSR = SI_{20min} of the liver / SI_{20min} of the spleen

3. Liver-spleen contrast ratio at 20 min after contrast media injection (LSC_N20) (81):

LSC_N20 = (SI_{20min} of the liver / SI_{pre} of the liver) / (SI_{20min} of the spleen / SI_{pre} of the spleen)

4. Liver-to-muscle ratio (LMR) (80):

LMR = SI_{20min} of the muscle / SI_{20min} of the muscle

5. Increase rate of LMR(ΔLMR) (82):

ΔLMR = (SI_{20min} of the liver / SI_{20min} of the muscle – SI_{pre} of the liver / SI_{pre} of the muscle) / (SI_{pre} of the liver / SI_{pre} of the muscle)

6. Hepatocellular uptake index (HUI)(83):

HUI = Liver volume × (SI_{20min} of the liver / SI_{20min} of the spleen -1)

7. Liver T1 relaxation time at 20min after contrast media injection ($T1_{20min}$):

$T1_{20min}$(liver) = 1 / ($1/T1_{pre}$ + ΔR1), the calculation of ΔR1 is described in reference (81) and the liver $T1_{pre}$ value was 586 ms (84).

8. Hepatic uptake rate (K_{hep}) (81):

K_{hep} = 0.39/20 × (($1/T1_{20min}$ of the liver -$1/T1_{pre}$ of the liver)/ ($1/T1_{20min}$ of the spleen -$1/T1_{pre}$ of the spleen)-0.77), where the intrinsic $T1_{pre}$ values of the liver and spleen were 586 ms and 1057 ms respectively (84).

DHCE-MRI derived parameters, including hepatic extraction fraction (HEF), mean transit time (MTT) and input-relative blood flow (irBF) were determined by deconvolutional analysis (85) using in-house developed software based on MATLAB® (Mathworks, Natick, MA).

Liver volumetry and its change

Liver volumetry in **Study I** was calculated by adding the volume of all voxels within the manually delineated liver borders (tVol). The "actual" liver volume was determined using the liver parenchymal part (excluding the vascular tissues) (pVol).

In **Study II**, the FLR was delineated along the Cantlie line using the preoperative HBP image and the FLR volume was semi-automatically calculated by using Volume Viewer software (Voxtool 11). The standardized FLR volume (sFLR-V) was calculated by:

$$\text{sFLR-V} = (\text{FLR volume} / \text{total estimated liver volume}) \times 100\%$$

in which the total estimated liver volume was determined by the formula: 1267*body surface area – 794(86).

The dynamic changes of FLR volume was calculated by: increFLR-V = (sFLR-V_{post} – sFLR-V_{pre}) / sFLR-V × 100%

The formula for the kinetic growth rate (KGR) of FLR volume (KGR-V) was: KGR-V = (sFLR-V_{post} – sFLR-V_{pre}) / time elapsed (week).

ICG-R15 test

In **Study II,** ICG-R15 test was conducted in the morning at the three time points. The dye ICG (Verdye®, Diagnostic Green GmbH, Aschheim-Dornach, Germany) was injected intravenously at a dosage of 0.5 mg/kg body weight and measured by the pulse spectrophotometry on the LiMON system (PULSION Medical System, Munich, Germany). The result of ICG retention test at 15 minutes after injection (ICG-R15, percentage, %) was used for liver function assessment.

Hepatobiliary scintigraphy exam

One hour after ICG-R15 test, HBS exam was carried out via intravenous injection of ^{99m}Tc-labeled iminodiacetic acid (200 MBq, ^{99m}Tc-mebrofenin, Bridatec®, GE Healthcare, Italy). The process can briefly be described as (87): after planar dynamic acquisitions to obtain the information of hepatic uptake function, a CT scan is performed for attenuation and anatomical correlation. A single photon emission computed tomography (SPECT) acquisition with projections can then be reconstructed using the software Hermes SUV SPECT Hybrid Recon™

FLR. To acquire a 3D assessment of liver function and functional liver volume, the SPECT acquisition is placed at approximately the peak of the hepatic time-activity curve. The FLR uptake rate of ^{99m}Tc-mebrofenin (FLR-F) is determined by multiplying the percentage of the total liver count. To eliminate individual metabolic differences, FLR-F is standardized by body surface area (sFLR-F, %/min/m^2)(23, 87). The FLR function changes (increFLR-F) and the KGR of the FLR function (KGR-F) are calculated as like that in liver volume, but using the sFLR-F.

Statistical Analysis

Continuous data with normal distribution are expressed as mean ± standard deviation and compared by Student's *t* test, while those with non-normal distribution are expressed as median and range and compared by Mann-Whitney *U* test. Categorical variables are presented as number (percentage). Spearman correlation analysis was applied to estimate the association between two variables and simple linear regression analysis to determine the association between liver function parameters and the clinical scoring systems. Repeated measures analysis of variation was exploited to evaluate the differences of variables at different time points. A two tailed p value less than 0.05 was regarded as statistically significant. Statistical analysis was performed by the R language software (Version 4.0.3, R Foundation for Statistical Computing, Vienna, Austria. https://www.R-project.org/).

4.3 Study III

Study design

This study was a systematic review. The research protocol was registered at the website PROSPERO (https://www.crd.york.ac.uk/prospero/, registration No. CRD42020200602) and the study was carried out in line with the guideline of the Preferred Reporting Items for Systematic Reviews and Meta-analysis (PRISMA) (88).

Literature search and study selection

A systematic literature searching strategy was performed in the four public databases: PubMed, Web of Science, Embase and the Cochrane Library until 11 December 2020. The key terms applied in the query included: "liver failure/dysfunction/insufficiency", "liver resection/hepatectomy" and "gadoxetic acid enhanced MRI".

English publications using a parameter derived from gadoxetic acid enhanced MRI for predicting PHLF in patients undergoing hepatectomy were included. Studies were ruled out if

they were 1) in the forms of review, conference abstract, letter, case report, experimental/animal research; 2) MRI only used for liver volume calculation; 3) there were other treatment between MRI exam and liver surgery, such as portal vein embolization. Study selection was performed by two researchers through scrutiny of the title/abstract first and then the full text for the uncertainty in a cross-validation way. Figure 3 describes the study selection process.

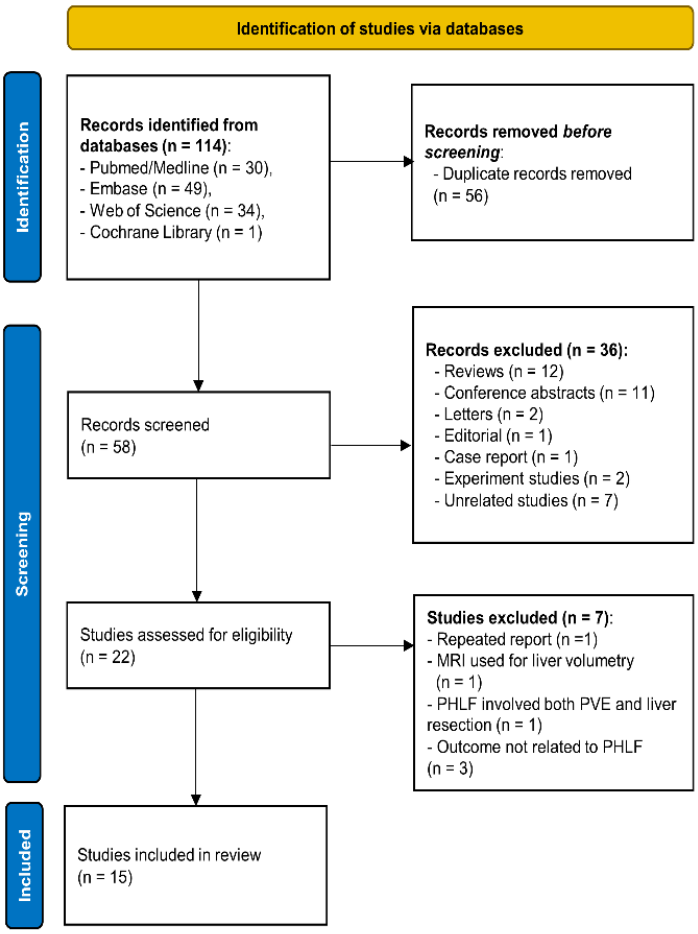

Figure 3. Flowchart of the study selection process.

Data collection

A predefined table was applied to extract the following information from the included studies by two independent investigators in consensus: 1) First author, publication year, country/region, study design, sample size, median/mean age, chronic liver disease status, main indications, extent of liver resection, PHLF criteria and PHLF incidence; 2) characteristics of the gadoxetic acid enhanced MRI derived parameters and their predictive performance; 3) ICG performance.

Risk of bias assessment

Research quality was appraised by using the Quality In Prognosis Studies (QUIPS) tool (89).

4.4 Study IV

4.4.1 Study design and patient

During the period between January 2017 and March 2019 at Southwest Hospital of Army Medical University, Chongqing, China, 276 consecutive patients who met the following criteria were included: 1) pathologically confirmed HCC; 2) preoperative gadoxetic acid enhanced MRI within four weeks before liver resection. Patients with antitumor therapy before liver resection (such as radiofrequency ablation), or with poor imaging quality were excluded. The eligible patients were randomly divided into training and test cohorts at a ratio of 7:3 according to random seed set by R software. Demographic and clinicopathological data were collected from the Hospital Information System and dichotomized according to commonly used thresholds (24, 90). Categorical data were expressed as number with frequency, and were compared by Chi-square test or Fisher's exact test, as appropriate. PHLF incidence followed the ISGLS criteria (71).

4.4.2 Pipeline of radiomics model development

The radiomics workflow of this study is described in Figure 4.

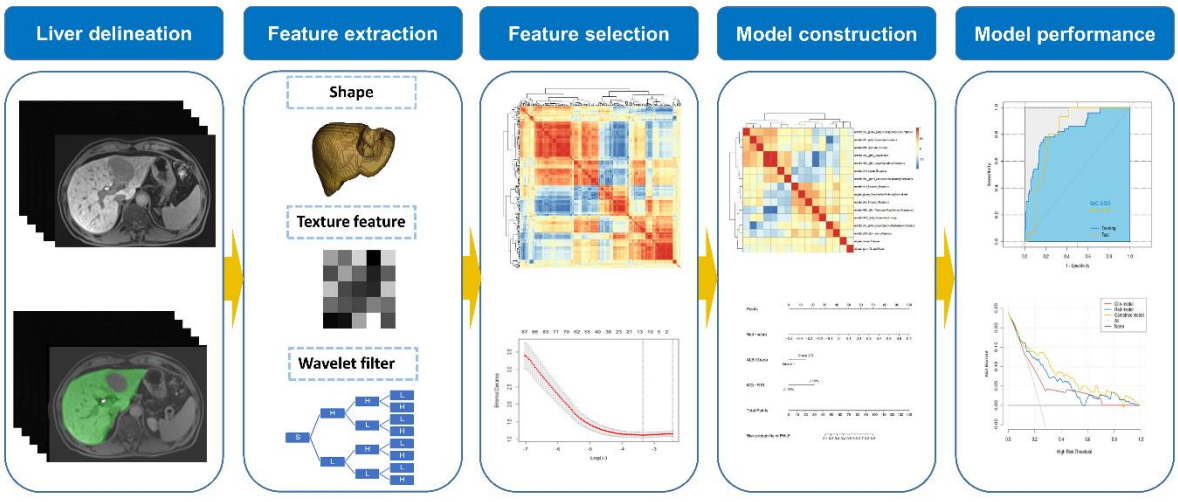

Figure 4. Workflow of radiomics model development

4.4.2.1 MRI acquisition and delineation of normal liver tissue

All patients underwent the MRI exam on a 3.0 T scanner (Magnetom Trio, Siemens Healthcare, Germany) with a standard scanning protocol. Pre- and dynamic contrast enhanced images were obtained through a T1 weighted three-dimensional volume interpolated breath hold sequence. The administration of gadoxetic acid was the same as in **Study I** and **II.** Images at hepatobiliary phase (HBP) were obtained at 15 min after contrast media injection (91). Manual delineation of the normal liver tissue (excluding the liver tumor) was performed on the hepatobiliary phase images using an open source software, ITK-SNAP (version 3.8.0 http://www.itksnap.org/).

4.4.2.2 Imaging preprocessing and feature extraction

Before feature extraction, all images were resampled to $1 \times 1 \times 1$ mm^3 via B-spline interpolation and the greyscale histogram was discretized to a bin width of 25. The package pyradiomics (version 3.0, https://github.com/AIM-Harvard/pyradiomics) was exploited to extract radiomics features from the delineated volume of interest (54). The features can be categorized into seven groups (92): (a) 2D/3D shape (n = 14); (b) first-order statistics (n = 18); (c) gray level co-occurrence matrix-derived feature (n = 24), (d) gray level run length matrix-derived feature (n = 16), (e) gray level size zone-derived feature (n = 16), (f) gray level dependence matrix-derived feature (n = 14); (g) neighbouring gray tone difference matrix feature (n = 5). These features were further transformed by the filter wavelet (n = 744). In total, 851 features were extracted.

To evaluate the agreement of extracted features, 30 patients were randomly selected and the non-tumorous liver was delineated by two researchers independently. The inter-observer agreement was evaluated by intraclass correlation (ICC) analysis. An ICC > 0.75 was set as a threshold representing parameters with good reproducibility and stability and those parameters were selected for further analysis (93, 94). After that, the delineation of the rest images was completed by one researcher.

4.4.2.3 Feature selection

All imaging features were then normalized by *z*-score to eliminate the impact of different units. The process of feature selection comprised two steps: in the first step, Spearman correlation analysis was performed among all parameters. When there were pairs with a high correlation

coefficient (> 0.99), one was randomly excluded from further analysis. In the second step, to avoid potential overfitting of the model, the screened features were further subject to the least absolute shrinkage and selection operator (LASSO) regression analysis to select the most informative features.

4.4.2.4 Model construction

4.4.2.4.1 Clinical model construction

Univariable logistic regression analysis was performed to detect clinicopathological risk factors associated with PHLF, with those *p* value less than 0.05 subject to multivariable logistic regression analysis for adjusting potential confounding. Clinical prediction model was built by linear combination of the significant risk factors in the multivariable regression analysis weighted by their corresponding coefficients.

4.4.2.4.2 Radiomics model construction

The radiomics features selected by LASSO algorithm was applied to develop a radiomics model by linear combination of the features (namely "Rad-model").

4.4.2.4.3 Combined model construction

Each patient was assigned a radiomics risk probability for PHLF (named "rad-score") according to the radiomics model. The rad-score together with the significant clinicopathological variables were used to construct a combined model. The optimal number of predictors in the combined model were determined via backward stepwise regression method with a minimum value of Akaike information criteria (AIC)(95).

4.4.2.5. Performance metrics of the model

The predictive performance of the models was evaluated by the area under the receiver operating characteristic curve (AUC). The optimal cut-off value of each model was calculated by Youden's index. Performance metrics including accuracy, sensitivity, specificity, positive predictive value and negative predictive value were determined for each model. A calibration curve was plotted to intuitively evaluate the consistency between the model predicted probability and the true probability, in which the diagonal represents an ideal situation, i.e the predicted probabilities equal to the real probabilities (96). Decision curve analysis was applied

to evaluate the clinical usefulness of the model (97). Statistical analysis and plotting was performed by the R software.

4.5 Ethical considerations

Study I was granted by the Regional Ethical Board in Stockholm (Regionala Etikprövningsnämnden i Stockholm) with permit number 04-721/1. Written informed consent was waived due to the retrospective nature of this study.

Study II was approved by the Regional Ethical Review Board and the Radiation Safety Committee at Karolinska University Hospital, Stockholm, Sweden (No. 2012/583-31/4). The study protocol was prospectively registered at https://clinicaltrials.gov under the identifier NCT03140917. Written informed consent was obtained from each patient before enrolment. The study was conducted in accordance with 1975 Declaration of Helsinki.

No ethics permit was required for **Study III** as it was a systematic review.

Research protocol of **Study IV** was approved by the Institutional Review Board of Southwest Hospital, Army Medical University, Chongqing, China (No. (B)KY2021068). Since it involved purely retrospective data analysis, written informed consent was not required.

5 RESULTS

5.1 STUDY I

There were two females in the CLD patients group and 10 females in the control group. The median age of the CLD patients was 57 years (range 43-61) and 33 years (range 22-45) for the healthy volunteers. For the patient group, median Child-Pugh score was 7 (range 5-12) and MELD score was (range 6-19).

Discriminative ability of MRI liver function parameters

All MRI liver function parameters but irBF had a statistically significant difference between CLD patient group and the control group ($p < 0.05$), implying a discriminative ability for CLD (AUC ranging from 0.79 to 1.00). There was a significant difference between CLD patients and the control groups for liver pVol ($p < 0.05$), but not for tVol ($p = 0.29$) (Table 4).

Table 4. MRI liver function parameters between two groups

	Patients	Controls	AUC	*p* value
Total liver volume (ml)	1496 (1037–1934)	1577 (1357–1886)	-	0.29
Parenchymal volume (ml)	1256 (915–1692)	1435 (1225–1774)	-	< 0.05
Total functional capacity (HEFml)	283 (112–412)	171 (53–341)	0.79	< 0.05
Global median HEF	0.22 (0.11–0.28)	0.09 (0.02–0.20)	0.94	< 0.05
Global median irBF	0.52 (0.43–0.63)	0.48 (0.31–0.74)	0.65	0.17
Global median MTT	789 (477–1318)	453 (203–686)	0.91	< 0.05
RLE	0.66 (0.47-0.81)	0.45 (0.24-0.65)	0.87	< 0.05
LSR	1.77 (1.45-1.92)	1.20 (0.79-1.82)	0.90	< 0.05
LSC_N20	1.41 (1.20-1.54)	1.23 (1.01-1.40)	0.85	< 0.05
LMR	2.34 (2.17-3.42)	1.69 (1.17-2.11)	1.00	< 0.05
ΔLMR	0.58 (0.48-0.87)	0.27 (0.12-0.55)	0.95	< 0.05
HUI-tVol	1039 (685-1523)	313 (-322-1441)	0.85	< 0.05
HUI-pVol	882 (590-1450)	291 (-301-1328)	0.87	< 0.05
$T1_{20min}$	0.24 (0.19-0.30)	0.31 (0.24-0.41)	0.87	< 0.05
K_{hep}	0.21 (0.09-0.40)	0.12 (0.03-0.23)	0.80	< 0.05

Note: AUC, area under receiver of characteristics; HEF, hepatic extraction fraction; HEFml, total liver functional capacity; HUI, hepatocellular uptake index, HUI-tVol calculated using total liver volume; HUI-pVol calculated using liver parenchymal volume; irBF, input-relative blood flow; K_{hep}, hepatic uptake rate; LMR, liver-to-muscle ratio; ΔLMR, Increase rate of Liver-to-muscle-ratio; LSC_N20, liver-spleen contrast ratio at 20min after contrast agent injection; LSR, liver-to-spleen ratio; MTT, mean transit time; RLE, relative liver enhancement; $T1_{20min}$, T1 at 20min after contrast agent administration.

Association between the MRI liver function parameters and clinical scoring systems

More than half of the MRI liver function parameters (8/13) showed a significant correlation with both the Child-Pugh score and MELD score, with correlation coefficients ranging from 0.66 to 0.91 ($p < 0.05$). Among those, LMR, LSR and HUI demonstrated not only the highest correlation coefficients but also excellent consistency with the two clinical scoring systems (Table 5).

Table 5. Correlation of MRI liver function parameters and clinical scores

	Child-Pugh score		**MELD score**	
	Spearman ρ	*p*-value	Spearman ρ	*p*-value
Total functional capacity (HEFml)	−0.72	< 0.05*	−0.76	< 0.05*
Global median HEF	−0.80	< 0.05*	−0.73	< 0.05*
Global median irBF	0.76	< 0.05*	0.55	0.10
Global median MTT	−0.26	0.46	0.05	0.88
RLE	−0.53	0.12	−0.61	0.06
LSR	−0.91	< 0.05*	−0.88	< 0.05*
LSC_N20	−0.66	< 0.05*	−0.71	< 0.05*
LMR	−0.91	< 0.05*	−0.86	< 0.05*
ΔLMR	−0.58	0.08	−0.68	< 0.05*
HUI-tVol	−0.91	< 0.05*	−0.88	< 0.05*
HUI-pVol	−0.91	< 0.05*	−0.88	< 0.05*
$T1_{20min}$	−0.52	0.12	−0.61	0.06
K_{hep}	−0.70	< 0.05*	−0.79	< 0.05*

Note: HEF, hepatic extraction fraction; HEFml, total liver functional capacity; HUI, hepatocellular uptake index, HUI-tVol calculated using total liver volume; HUI-pVol calculated using liver parenchymal volume; irBF, input-relative blood flow; K_{hep}, hepatic uptake rate; LMR, liver-to-muscle ratio; ΔLMR, Increase rate of Liver-to-muscle-ratio; LSC_N20, liver-spleen contrast ratio at 20min after contrast agent injection; LSR, liver-to-spleen ratio; MELD score, Model for End-stage Liver Disease score; MTT, mean transit time; RLE, relative liver enhancement; $T1_{20min}$, T1 at 20min after contrast agent administration.

Correlations between the three categories of MRI liver function parameters

When not taking irBF into account, a good inherent consistency was observed within each category of liver function parameters (0.60 - 0.97 within SI-derived parameters, 0.71 for T1 relaxometry derived parameters and 0.50 - 0.76 for DHCE-MRI derived parameters, all $p < 0.05$).

The correlations between SI-derived parameters and T1 relaxometry derived parameters ranged from 0.60 to 1.00 ($p < 0.05$), those between SI-derived parameters and DHCE-MRI derived parameters from 0.38 to 0.74 ($p < 0.05$) and those between T1 relaxometry derived parameters and DHCE-MRI derived parameters from 0.38-0.61 ($p < 0.05$).

RLE showed a perfect correlation with $T1_{20min}$ ($|r| = 1.00$, $p < 0.05$) while irBF was only significantly correlated with HEFml ($|r| = 0.38$, $p < 0.05$) (Figure 5).

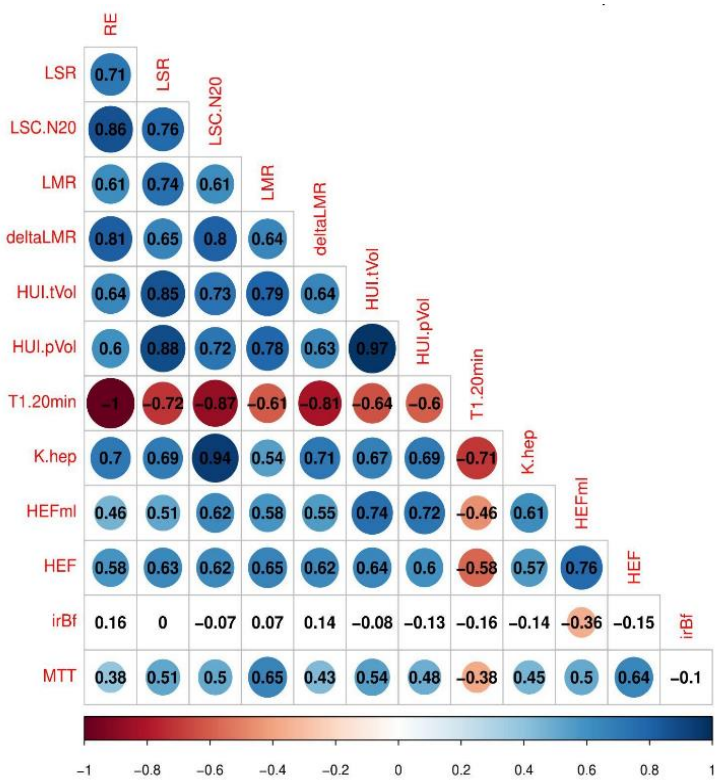

Figure 5. Correlation coefficients between parameters derived from gadoxetic acid enhanced MRI. *Note: HEF, hepatic extraction fraction; HEFml, total liver functional capacity; HUI, hepatocellular uptake index, HUI-tVol calculated using total liver volume; HUI-pVol calculated using liver parenchymal volume; irBF, input-relative blood flow; K_{hep}, hepatic uptake rate; LMR, liver-to-muscle ratio; ΔLMR, Increase rate of Liver-to-muscle-ratio; LSC_N20, liver-spleen contrast ratio at 20min after contrast agent injection; LSR, liver-to-spleen ratio; MTT, mean transit time; RE, relative enhancement of the liver; $T1_{20min}$, T1 at 20min after contrast agent administration.*

5.2 STUDY II

The 10 patients with CRLM enrolled in this study had a median age of 63 (44-75) years and a male/female ratio of 7:3. No patient developed PHLF or biliary leakage after liver resection.

Consistency between the three modalities in liver function evaluation

At baseline exam, the five MRI derived parameters showed a good consistency, with correlation coefficients ranging from 0.69 to 0.83 ($p < 0.05$). ICG-R15 exhibited a significant correlation with LMR ($r = 0.66$, $p < 0.05$). There were significant correlations between sFLR-F and LSR, and between sFLR-F and K_{hep} ($r = -0.71$, -0.70 respectively, both $p < 0.05$) (Figure 6).

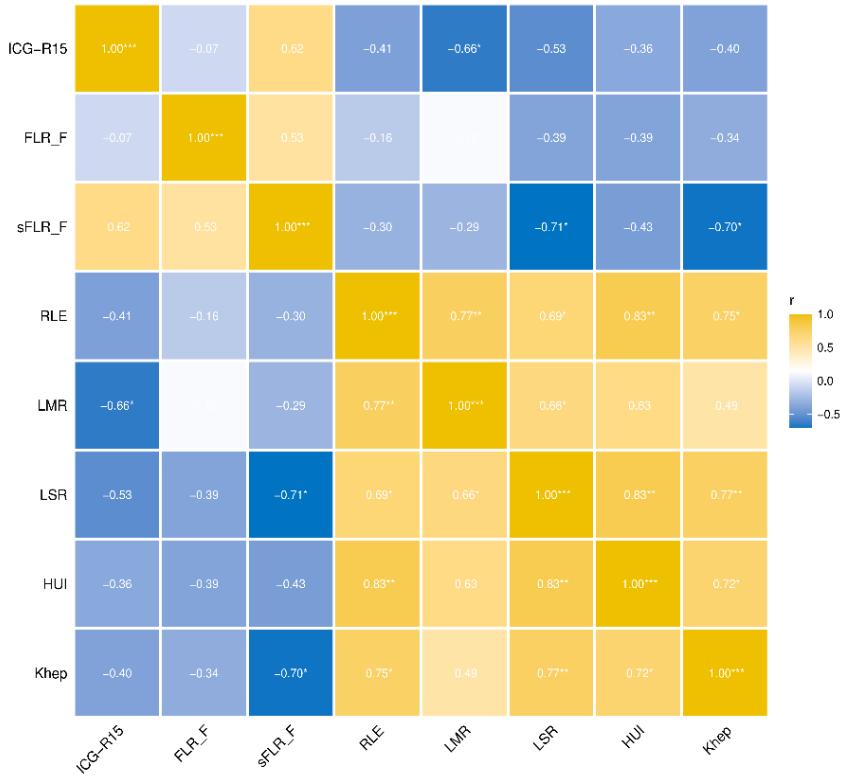

Figure 6. Correlation coefficients between liver function parameters. *Note: HUI, hepatic uptake index; ICG-R15, indocyanine green retention test at 15 min; FLR-F, corrected mebrofenin uptake rate in FLR (%/min/m²); K_{hep}, hepatic uptake rate; LMR, liver-to-muscle ratio; LSR, liver-to-spleen ratio; RLE, relative liver enhancement; sFLR-F, standardized FLR-F. * p <0.05, ** p<0.01, *** p<0.001.*

Dynamic changes of liver volume and function

The FLR related parameters (FLR-F, sFLR-F, FLR volume and sFLR-V) showed a significant difference among the three time points, while no significant difference was observed among the other liver function parameters at these three time points.

The difference of increase rate of liver volume and function at POD7 and POD28 was not significant (both $p > 0.05$), while the differences of the KGR of liver volume and function during POD1-7 and POD1-28 were significant (both $p < 0.05$). There were not significant differences between liver volume and function in the first week after hepatectomy, and that at first month after hepatectomy. Detailed description of the liver volume and function changes is provided in Table 6.

Table 6. Liver function and volume at the three time points

Parameter	Preoperative	POD7	POD28	*p* value
ICG-R15 (%)	7.9 (0.4-14.7)	11.1 (1.2-23.3)	8.3 (3.9-21.0)	0.599
Hepatobiliary scintigraphy				
FLR-F (%/min/m2)	3.1 (2.3-4.7)	5.5 (4.1-7.9)	6.6 (5.2-7.7)	< 0.001
sFLR-F (%)	36(25-48)	65(44-93)	75(56-94)	< 0.001
Gadoxetic acid enhanced MRI				
RLE	0.66 (0.48-1.16)	0.74 (0.28-0.96)	0.75 (0.56-0.92)	0.708
LMR	2.04 (1.50-2.49)	1.78 (1.43-2.30)	2.04 (1.88-2.43)	0.221
LSR	1.95 (1.26-2.67)	1.77 (1.29-2.54)	2.04(1.77-2.56)	0.303
HUI	496 (202-870)	763 (373-1665)	1343 (921-1525)	0.001
K_{hep}	0.14 (0.07-0.33)	0.16 (0.01-6.46)	0.16 (0.06-0.27)	0.919
FLR volume (ml)	546 (377-772)	1039 (744-1307)	1194 (971-1404)	< 0.001
sFLR-V (%)	38 (29-53)	69 (55-81)	79 (66-90)	< 0.001
FLR increase rate				
increFLR-F (%)		92 (13-152)	99 (62-214)	0.307#
increFLR-V (%)		79 (37-134)	87 (66-179)	0.315#
		Interval POD 1-7	**Interval POD 1-28**	
Kinetic growth rate				
KGR-F (%/week)		31(5-45)	10 (6-13)	< 0.001#
KGR-V (%/week)		30 (19-47)	9 (6-13)	0.003#

Note: Data are expressed as median with range. P values are calculated by Kruskal-Wallis test unless otherwise specified. # compared by the Mann Whitney U test. HUI, hepatic uptake index; ICG-R15, indocyanine green retention test at 15 min; increFLR_F, FLR increase rate in function; increFLR_V, FLR increase rate in volume; FLR, future liver remnant; FLR-F, corrected mebrofenin uptake rate in FLR (%/min/m^2); KGR-F, kinetic growth rate in function; KGR-V, kinetic growth rate in volume; K_{hep}, hepatic uptake rate; LMR, liver-to-muscle ratio; LSR, liver-to-spleen ratio; POD, postoperative day; RLE, relative liver enhancement; sFLR-F, standardized FLR-F; sFLR-V, standardized FLR volume

Liver function parameters for prediction of liver growth after hepatectomy

LMR and ICG-R15 showed a significant correlation with increFLR-V and KGR during the first week after hepatectomy (|r| range 0.67-0.84, $p < 0.05$), while HUI has a significant correlation with increFLR-F and KGR-F during the first week after hepatectomy ($r = 0.84, 0.87$ respectively, both $p < 0.05$). There was also a significant correlation between LSR and increFLR-F at POD7 ($r = 0.79$, $p < 0.05$).

Table 7. Correlation coefficients between the three modalities and the future liver remnant dynamic changes in volume and function in the first week after hepatectomy

	ICG-R15	FLR-F	sFLR-F	RLE	LMR	LSR	HUI	Khep	sFLR-V
increFLR-F	-0.50	-0.65*	-0.72*	0.60	0.43	0.79**	0.84**	0.63	-0.24
increFLR-V	-0.67*	0.03	-0.61	0.44	0.75*	0.59	0.32	0.59	-0.72*
KGR-F	-0.27	-0.53	-0.31	0.52	0.38	0.60	0.87**	0.38	0.01
KGR-V	-0.69*	0.20	-0.28	0.57	0.84**	0.38	0.44	0.42	-0.22

*Note: FLR, future liver remnant; FLR-F, corrected mebrofenin uptake rate in FLR (%/min/m2); HUI, hepatic uptake index; ICG-R15, indocyanine green retention test at 15 min; increFLR_F, FLR increase rate in function; increFLR_V, FLR increase rate in volume; KGR-F, kinetic growth rate in function; KGR-V, kinetic growth rate in volume; Khep, hepatic uptake rate; LMR, liver-to-muscle ratio; LSR, liver-to-spleen ratio; RLE, relative liver enhancement; sFLR-F, standardized FLR-F; sFLR-V, standardized FLR volume. * p <0.05, ** p<0.01.*

5.3 STUDY III

Study and patient characteristics

A total of 15 studies published between August 2011 and September 2020 were included in the systematic review (98-112). In total, there were 1327 patients included, with sample size ranging from 11 to 192. All but one were retrospective studies and five stated whether their subjects were consecutive or not. The average age in the included studies ranged from 49 to 72 years. Five studies evaluated PHLF exclusively on hepatocellular carcinoma cases. Eight studies focused on patients undergoing major hepatectomy (defined as more than three Couinaud segments) while the remaining had not such restriction. The ISGLS criteria of PHLF was applied by 14 studies and the incidence of PHLF ranged from 3.9% to 40%. Table 8 gives more details about the included studies. Most studies showed a low-to-moderate risk of bias in each domain within the QUIPS tool.

MRI liver function parameters and its performance in prediction of PHLF

A majority of studies (13/15) applied SI-based parameters for PHLF prediction; only one study used DHCE-MRI derived parameters and one study radiomics approach. Among the 13 SI-based studies, RLE or RLE-based parameters were applied in around half of them (7/13). Seven studies evaluated a compound parameter which integrated liver volume and SI derived parameters. HUI, a typical compound parameter, was adopted in four studies for PHLF prediction. Eight studies quantified the liver function on the FLR part while five studies on the whole liver (Table 9).

The AUC, reported in 13 studies, ranged from 0.67 to 0.96 and the accuracy, reported in four studies, from 0.80 to 0.88. The sensitivity and specificity varied from 75% to 100% and from 54% to 93% respectively among 11 studies (Table 9).

Efficacy of MRI and ICG test in prediction of PHLF

The predictive power of ICG test or ICG-based parameter in estimation of PHLF was reported in 11 studies, among which only 5 studies reported a significant result. Three out of these five studies provided AUC of the ICG test or ICG-based parameter in prediction of PHLF, ranging from 0.75 to 0.78.

Table 8. Study and patient characteristics of the included studies

Study ID	Year	Study design	Sample size	Age	Chronic liver disease	Main indications‡	Extent of liver resection	Cases of PHLF (%)
Cho2011	2011	R	29	57	48%(cirrhosis 21%)	HCC (48%)	major§	7(24%)
Wibmer2013	2013	R	73	64.4	NA	CRLM(71%)	major	3(4%); 29(40%)
Sato2015	2015	R	11†	59.5	NA	Liver metastases (52%)	major	7(waived)
Jin2016	2016	R	121	56	92%(cirrhosis 61%)	HCC(100%)	minor§ + major	7(5.8%);38(31%)
Costa2017	2017	R	65	60.8	NA	CRLM(71%)	major	9(14%)
Asenbaum2018	2018	R	62	59.8	NA	CRLM(53%)	major	16(26%)
Chuang2018	2018	R	115	60	100%	HCC(78%)	minor + major	16(14%)
Kim2018	2018	R	73	59.7	100%(cirrhosis 47%)	HCC(100%)	minor +major	18(25%)
Theilig2019	2019	P	36	62	NA	CRLM(31%);HC(31%)	major	14(39%)
Araki2020	2020	R	155	67	NA	Liver metastases (43%)	minor+major	9(6%)[#]
Donadon2020	2020	R	137	65	18%	CRLM (77%)	minor + major	22(16%)
Orimo2020	2020	R	192	65/72	NA	HCC(69%)	major (≥ 2 sections)	49(26%)
Zhu2020	2020	R	101	55(M),53(F)	100%(cirrhosis 23%)	HCC(100%)	major	15(15%) ¶
Tsujita2020	2020	R	41	66	66%	HCC(100%)	major + minor	16(39%)
Wang2020	2020	R	116	49.0	86% (cirrhosis 62%)	HCC(100%)	major + minor	28(22%)

Note: † the number of patients for a second analysis; ‡ the most frequent indication with its percentage is listed while the exclusive indication is marked as 100%; § "major liver resection" refers to three or more Couinaud segments, while "minor liver resection" to less than three Couinaud segments; ¶posthepatectomy liver failure is defined as encephalopathy, with hyperbilirubinemia (total bilirubin > 4.1 mg/dL), international normalized ratio > 2.5, and ascites with drainage volume > 500 mL/d; # refers to the incidence of PHLF Grade B, C, in which clinical management after operation is altered while it remains the same in Grade A of PHLF; CRLM, colorectal liver metastases; HC, Hilar cholangiocarcinoma; HCC, hepatocellular carcinoma; NA, not available; P, prospective study; PHLF, post-hepatectomy liver failure; R, retrospective study.

Table 9. Summary of gadoxetic acid-enhanced MRI derived parameters in prediction of post-hepatectomy liver failure

Study ID	Quantitative parameter	Quantified liver region	Formula	AUC (95% CI)
Cho 2011	RLE and remRLE	Whole and FLR	$(SI_{HBP} - SI_{pre})/SI_{pre}$	0.84
Wibmer2013	RLE(%)	Whole	$(SI_{HBP} - SI_{pre})/ SI_{pre} * 100$	NA
Sato2015	remRE Index	FLR	$(SI_{HBP} - SI_{pre})/ SI_{pre} * 100 *$ remLV	NA
Jin2016	RLE(%)	Whole	$(SI_{HBP} - SI_{pre})/ SI_{pre} * 100$	0.79 (0.65-0.92)
Costa2017	RLE	Whole	$(SI_{HBP} - SI_{pre})/ SI_{pre}$	0.67
Asenbaum2018	functFLR	FLR	(FLR(%)*remRLE)/body weight	0.90(0.80-0.98)
Chuang2018	remCER	FLR	$(SI_{HBP} - SI_{pre})/(SI_{TP} - SI_{pre})$	0.78(0.69-0.85)
Kim2018	rHUI-BW	FLR	remLV * $((remSI_{L20} / SI_{S20}) - 1)$/body weight * 1 000	0.96(0.88-0.99)
Theilig2019	remRLE	FLR	$(SI_{HBP} - SI_{pre})/ SI_{pre}$	0.85
Araki2020	FRLV_LMR	FLR	$((remSI_{L20} / remSI_{Lpre})/(SI_{M20} / SI_{Mpre})$*remLV) /BSA	0.94†(0.89-0.99) (SCoh)
Donadon2020	HUI	Whole	LV*$(SI_{L20} / SI_{S20} - 1)$	0.84(0.71-0.92)
Orimo2020	rHUI-BSA	FLR	remLV * $((remSI_{L20} / SI_{S20}) - 1)$/BSA	0.80(SCoh)
Zhu2020	Radiomics	Whole	NA	0.90 (0.82-0.96)
Tsujita2020	rHUI and HUI	FLR and resected liver	rHUI = remLV * $((remSI_{L20} / SI_{S20}) - 1)$; HUI = rHUI+((TFLV-remLV)* $((resSI_{L20} / SI_{S20}) - 1)$)	0.96 (0.91-1.00)†
Wang2020	RF_{UR}, sRF_{UR}	FLR	NA (based on dynamic contrast enhanced MRI)	0.88 (0.81-0.93)

Note: AUC, area under the receiver operating characteristic curve; BSA, body surface area; FLR, future liver remnant; FRLV(LMR), functional remnant liver volume corrected by liver-muscle ratio; functFLR, functional FLR; HUI, hepatic uptake index; LV, liver volume; NA, not available; remCER, contrast enhancement ratio of the liver remnant; remLV, the remnant liver volume; remRE Index, relative enhancement index of the liver remnant; remRLE, relative liver enhancement of the liver remnant; $remSI_{Lpre}$, signal intensity of the liver remnant before contrast medium injection; $remSI_{L20}$, signal intensity of the liver remnant at 20 min after contrast medium injection; $resSI_{L20}$, signal intensity of the resected liver at 20 min after contrast medium injection; rHUI, hepatic uptake index of the liver remnant; rHUI-BSA, rHUI corrected by BSA; rHUI-BW, rHUI corrected by body weight; RF_{UR}, sum of the uptake rate of the remnant liver regions; RLE, relative liver enhancement; SI_{HBP}, liver signal intensity in hepatobiliary phase; SI_{L20}, signal intensity of the liver at 20 min after contrast medium injection; SI_{M20}, signal intensity of the muscle at 20 min after contrast medium injection; SI_{Mpre}, signal intensity of the muscle before contrast medium injection; SI_{pre}, liver signal intensity before contrast medium injection; SI_{S20}, signal intensity of the spleen at 20 min after contrast medium injection; SI_{TP}, liver signal intensity in transitional phase; sRF_{UR}, sum of the uptake rate of the remnant liver standardized by standard liver volume; TFLV, total functional liver volume.

5.4 STUDY IV

Among the included 276 subjects, 238 were males and 38 females, and most were aged more than 55 years old (71.4%). A total of 65 patients developed PHLF, accounting for 24% of the whole cohort. The training and test cohorts were randomly assigned to 194 and 82 patients, respectively. The demographic and clinicopahological characteristics between the training and test cohorts were balanced.

Development of the clinical model

At uni- and multivariable logistic regression analysis, three clinicopathological factors were detected to be significantly correlated with PHLF, i.e. platelet, ALBI grade and ICG-R15 ($p < 0.05$) (Figure 7). The Clin-model was developed by these three factors, and the formula was:

$$Y = -1.66 - 0.92*\text{Platelet} + 1.162*\text{ALBI grade} + 1.58*\text{ ICG-R15}$$

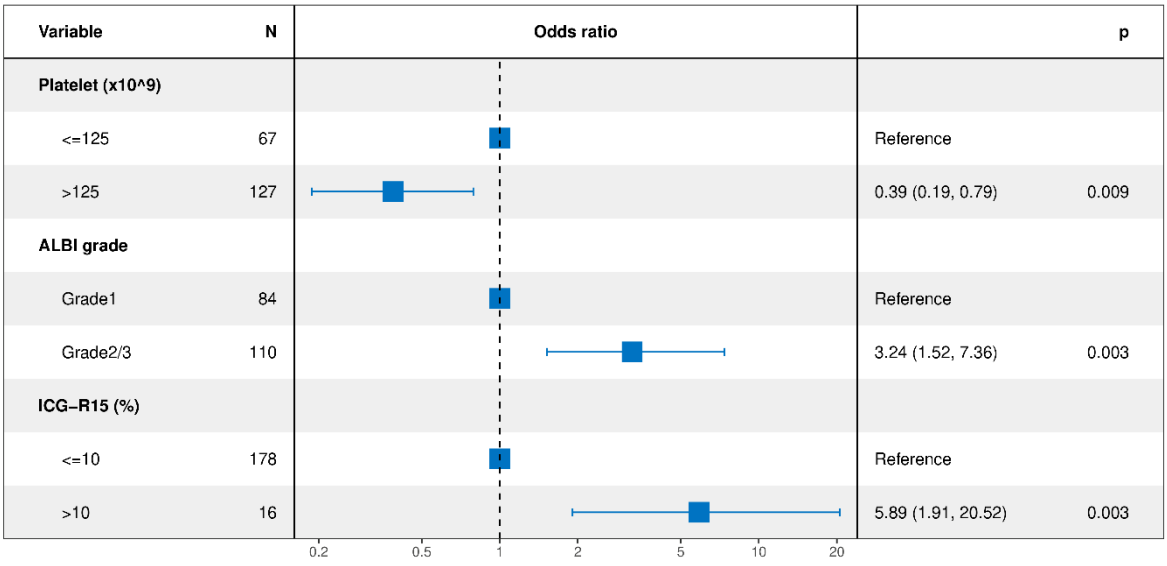

Figure 7. Forest plot shows the odds ratio of the three significant variables at multivariable regression analysis. *Note: ALBI grade, albumin-bilirubin grade; ICG-R15, indocyanine green retention test at 15 min.*

Imaging feature selection and development of the radiomics model

Among the 851 features, 494 (58%) reproducible and stable features remained after removal of features with ICC less than 0.75. In the two-step feature selection process, 315 features were left after screening out redundant features by Spearman correlation analysis. These 315 features were further subject to LASSO algorithm and 16 features with non-zero coefficients were finally selected for modelling (Rad-model) (Figure 8).

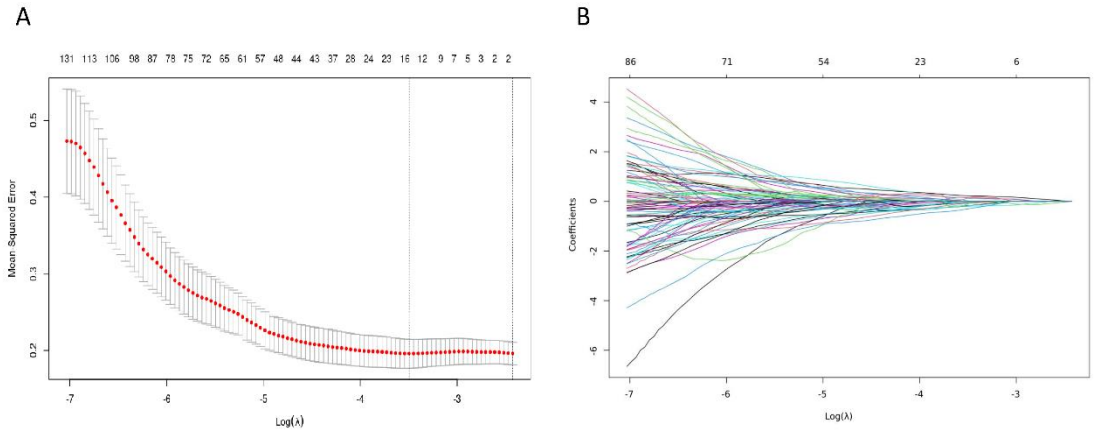

Figure 8. Feature selection process in the algorithm least absolute shrinkage and selection operator (LASSO). *A. The super-parameter λ was determined by the minimum of mean-squared error in 5 fold cross-validation way. B. The LASSO path plot shows the different coefficients of the variables in the model with λ trending to zero.*

Development of the combined model

The three independent risk factors and the rad-score, which was derived from the Rad-model, were used to construct a compound model. The ideal one, selected by the AIC minimum value, consisted of three variables: ALBI grade, ICG-R15 and rad-score. It was visualized as a nomogram for facilitating clinical usage (Figure 9).

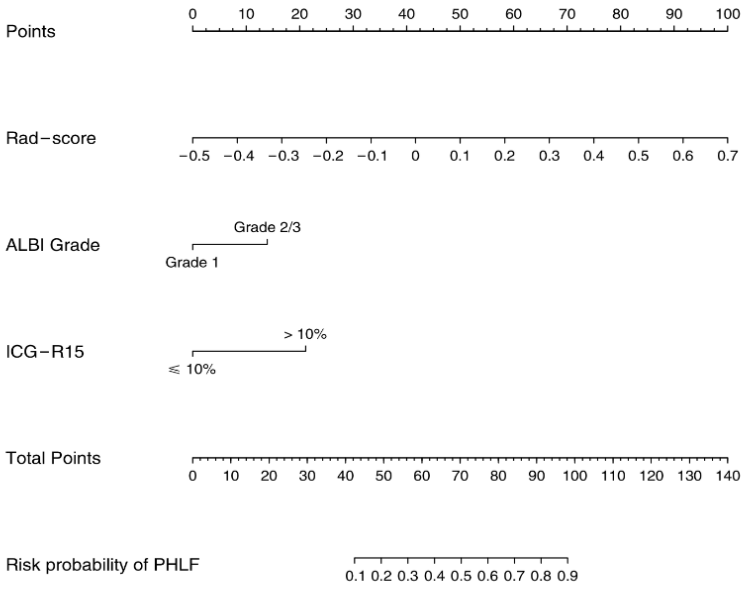

Figure 9. A radiomics based nomogram for prediction of post-hepatectomy liver failure (PHLF). *Note: ALBI grade, albumin-bilirubin grade; ICG-R15, indocyanine green retention test at 15 min.*

Model performance

The AUC of the Clin-model, Rad-model and the combined model were 0.74 (95%CI: 0.65-0.73), 0.79(95%CI: 0.72-0.86) and 0.84(95%CI: 0.77-0.90) respectively in the training cohort and 0.71(95%CI:0.57-0.84), 0.79 (95%CI:0.69-0.89) and 0.82(95%CI:0.72-0.91) in the test cohort (Figure 10 A). Given the combined model possessed a highest AUC in the test cohort, it was chosen as the PHLF prediction model. The optimal cut-off value of the combined model was 0.28 and the accuracy, sensitivity, specificity, positive predictive value and negative predictive value were 0.72, 0.93, 0.67, 0.39, 0.98 respectively.

At decision curve analysis, the combined model demonstrated a better clinical usefulness than the other two models (Figure 10 B). The calibration curve showed a good agreement between the combined model predicted events and the actual events with a bootstrapping of 1000 times (Figure 10 C, D).

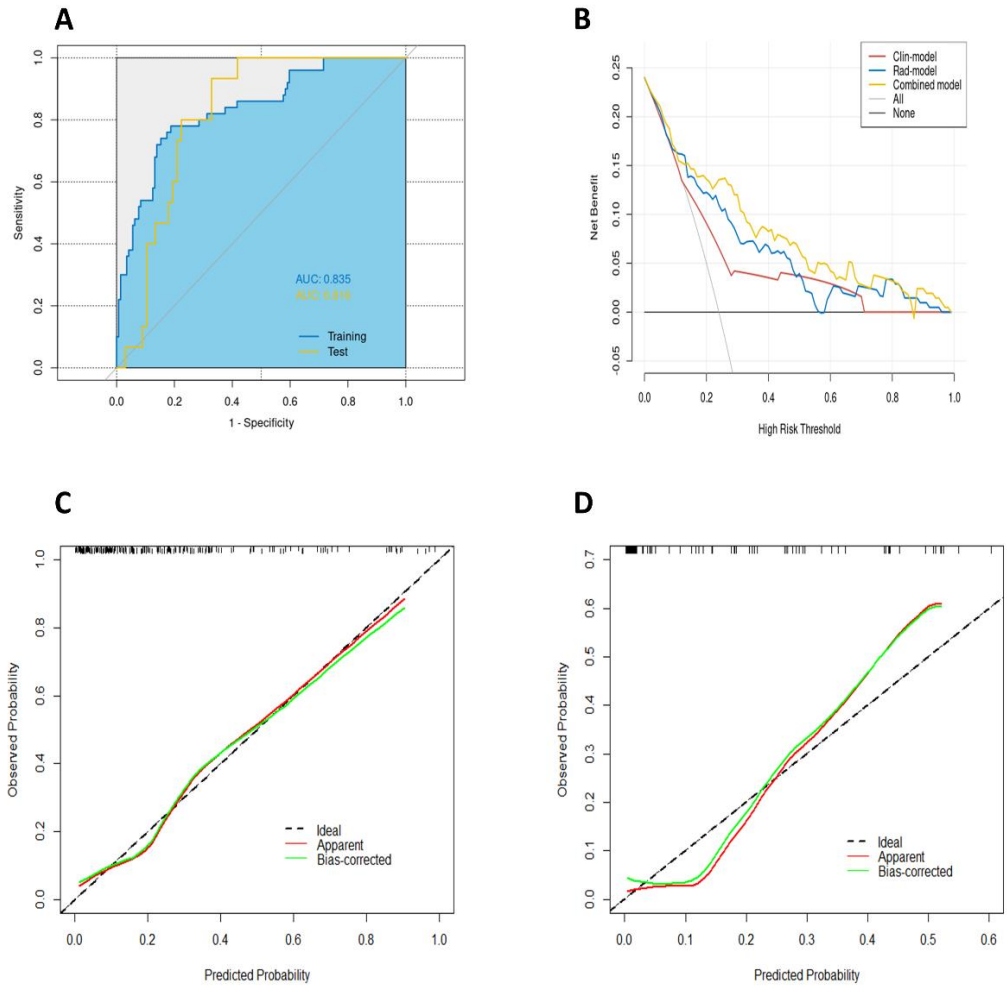

Figure 10. Performance of the prediction models for post-hepatectomy liver failure. *A. Area under the receiver operating characteristic curve of the combined model in the training and test cohorts. B. Decision curve analysis of the Clin-model, Rad-model and the combined model.* C. *Calibration curves of the combined model in the training cohort. D. Calibration curves of the combined model in the test cohort.*

6 DISCUSSION

6.1 GENERAL DISCUSSION ABOUT STUDY I AND II

Both **Study I and II** consistently supported that LMR can serve as a reliable and effective parameter for liver function evaluation both in patients with chronic liver disease and with CRLM. It did not only discriminate chronic liver disease from the normal, but also correlated closely with Child-Pugh score, MELD score, ICG-R15, and FLR volume and function increase. Besides, its calculation only involved the placement of ROIs on the liver and muscle in a single contrast agent phase which enables an easy clinical implementation. The value of this parameter is worth further confirmation in multicenter studies with large study populations. By contrast, there was no significant correlation between RLE and any of Child-Pugh, MELD score, ICG-R15, FLR volume or function increase in neither of the studies, although RLE is the most commonly used parameter in the current literature.

Liver regeneration capacity reflects an important aspect of liver function (113-115). Liver regeneration prediction using MRI can thereby have a crucial influence on the treatment of patients with liver malignancy (116-118). This point is especially essential in the setting of portal vein embolization, among which as many as 20-40% of patients cannot proceed to curative liver resection due to insufficient FLR growth (119-121). The other way around, when a patient has a marginally sufficient FLR for liver resection, but the preoperative assessment shows a good liver growth potential, the risk of PHLF is small, and the patient can be eligible for curative treatment. Thus, if liver regeneration ability can be estimated before treatment, the patient management can be optimized and personalized (122). Our results showed that among the three modalities (ICG, HBS and gadoxetic acid enhanced MRI) the latter has the greatest potential for estimation of the liver regeneration capacity.

The consistency among ICG-R15, HBS and gadoxetic acid enhanced MRI in evaluation of liver function was confirmed in **Study II** and can be interpreted by the fact that they have a similar transporter pathway into the hepatocytes (23). The good consistency suggests that one modality may substitute for the other when one is contraindicated. Given the fact that gadoxetic acid enhanced MRI is a common exam in detection and characterization of liver tumors, it seems possible for gadoxetic acid enhanced MRI to supply both anatomical information and the liver function information as a “one-stop-shop”. Furthermore, MRI does not involve radiation exposure, making it more acceptable for patients.

The main limitation of both **Study I and II** was the small sample size, which may undermine the reliability of the findings, although **Study II** was prospectively designed. However, these studies were primarily designed as pilot studies, with one of the aims to supply a basis for power analysis for future studies with large sample size. Secondly, neither of the studies evaluated the correlation between the liver function parameters and the clinical events, such as PHLF. A confirmation of our findings in the real-world practice is necessary.

6.2 GENERAL DISCUSSION ABOUT STUDY III AND IV

With pooling analysis of 15 studies, the systematic review showed that gadoxetic acid enhanced MRI had a high capacity for PHLF prediction, suggesting it to be a promising imaging biomarker for identification of patients with high risk of PHLF.

Among the included 15 studies, a majority of the gadoxetic acid enhanced MRI derived parameters belonged to the SI-derived category, probably as they were simple, understandable and accessible methods. However, these parameters were limited by their arbitrary character, making it impossible to compare them between different medical centers. T1 relaxometry related parameters can objectively reflect the intrinsic tissue property, being independent from the scanning devices and field strength (48, 123-125). This seems to be a reliable approach to predict PHLF. Nevertheless, there have not been any studies using T1 relaxation time based parameters for PHLF prediction published yet.

Even in the category of SI-based parameters, an obvious heterogeneity existed. Firstly, to overcome the influence of MRI scanner and coils, SI-based parameters are often corrected by intrinsic tissues, such as spleen, muscle or the baseline SI value of the liver. Among them, due to its simplicity, RLE was the most widely used parameter. However, according to the outcome of **Study I and II**, it does not seem to be a reliable and stable parameter. Secondly, the measured regions were different: some studies focused on the FLR part, while the others measured the whole liver. Theoretically, the former should have a better accuracy in prediction of PHLF. Thirdly, as liver volume is a basis and surrogate of liver function evaluation, some researchers proposed a compound parameter by integrating SI-based parameter and the liver volume (for instance, HUI). Lastly, the obtained MRI liver function parameter was further corrected by body weight or body surface area in some studies, considering the heterogeneity in body size among individuals. This variability in reporting the SI liver function parameter

created a barrier for comparison across different studies and it was also not possible to synthesize the results to evaluate its pooled performance.

As the ICG test often serves as a reference standard in quantitative evaluation of liver function (31, 32, 126, 127), we additionally made a comparison between the ICG test and the gadoxetic acid enhanced MRI in prediction of PHLF. It turned out that less than half studies (5/11) showed a significantly predictive value of ICG test, inferior to MRI.

There are some limitations in **Study III** to be acknowledged. 1) the number of eligible studies was limited: among them only one was prospectively designed, only six studies had sample size more than 100 patients, and only two studies included both development cohort and evaluation cohort. More studies are required to draw a convincing conclusion. 2) when detecting risk factors associated with PHLF, not all studies evaluated sufficient clinical variables at their regression analysis. It has been well recognized that some surgery-related factors are independent indicators for PHLF (73), but these factors were often ignored. 3) More attention should also be paid on the reporting norm to make the results reproducible and repeatable by other researchers.

The systematic review also revealed that novel approaches have emerged for liver function evaluation and PHLF prediction, such as radiomics and machine learning techniques. We therefore designed **Study IV** to test our hypothesis that radiomics features from hepatobiliary phase can be applied to construct a prediction model for PHLF estimation. The developed model demonstrated a high discriminative ability in both training and test cohorts with AUCs of 0.84, 0.82 respectively.

ICG-R15 was one of the elements in our prediction model as it was robust and independent at both uni- and multivariable regression analyses. Its odds ratio was 4.9 after adjusting for confounders. While most studies in **Study III** did not detect ICG test as an independent parameter (98, 101, 103, 104, 107, 109), the predictive value of the ICG test for PHLF estimation still requires further investigation (128).

Another clinical variable in the model was ALBI grade, which integrated two serum biochemical tests (albumin and bilirubin). This parameter was proposed to overcome the subjectivity of Child-Pugh system and it has been proven to be a reliable and accurate index for liver function evaluation in HCC (27, 129). The odds ratio of ALBI grade in our study was 3.2, which was consistent with that of Xiang's study (130). Interestingly, neither Child-Pugh score nor MELD score were independent indicators for PHLF estimation in our cohort.

Rad-score, which was calculated by the radiomics model, showed a high capacity for PHLF prediction. It was composed of 16 radiomics features in which a majority belonged to wavelet-related features. The filter wavelet seems to be a powerful tool in decomposition of original images and better demonstrates heterogeneity of the tissue (131). This result supports our hypothesis that hepatobiliary phase of gadoxetic acid enhanced MRI contains information for liver function evaluation.

There were some limitations in **Study IV.** First, the patient data was collected at a single institution in a retrospective manner, in which the selection bias may be inevitable. As lacking external validation cohort, the generalization of the model still needs further evaluation. Second, the radiomics features were extracted from the whole normal hepatic tissue, not just the FLR part. Whether there is difference in model performance between these two volumes warrants future research to elucidate.

7 CONCLUSIONS

Based on the findings of the four studies the following conclusions can be drawn:

Study I

- Simple parameters derived from SI showed a similar performance in evaluation of liver function to those based on complex techniques, such as DHCE-MRI.
- For clinical routine usage, LMR (an SI-based parameter) seems to be an easy-to-use parameter for preoperative liver function assessment.

Study II

- The dynamic change of the liver function was parallel with that of the liver volume during the first month after hepatectomy in patients with CRLM.
- LMR and HUI seems to be reliable parameters in evaluation of liver function and for prediction of liver growth after hepatectomy.

Study III

- Gadoxetic acid enhanced MRI showed a high predictive ability in prediction of PHLF and can potentially serve as a reliable and accurate imaging biomarker.

Study IV

- The prediction model integrating ICG-R15, ALBI grade and rad-score was developed and internal validated. It showed to be an accurate and reliable imaging signature in stratifying patients into different levels of risk for PHLF, and can serve as a decision aid in surgery treatment planning.

8 POINTS OF PERSPECTIVE

There are some remaining issues in this thesis which require future research to address.

To begin with, prospective studies with large sample size and heterogeneous patient population from multicenter are warranted to verify our findings. Before translating it into clinical utility, our radiomics model needs external validation to test its robustness.

Confounders at SI measurement should be further identified and corrected. Currently, SI values are measured after administration of gadoxetic acid at 0.025 mmol/kg or 0.1 mL/kg. However, that ignores the impact of body weight variations. That is to say, a thin patient with poor liver function may have a similar SI value as an overweight patient with a normal liver function. This factor was neglected by most studies.

Another direction goes to the regional assessment of liver function, i.e. the FLR part. Although gadoxetic acid enhanced MRI has shown a potential to evaluate liver function of FLR, it just uses several ROIs at a certain cross-section slice, which might not fully reflect the liver function. With the assistance of artificial intelligence, automatic segmentation of the FLR and extraction of the textual information would provide insights into comprehensive and accurate evaluation of the FLR function.

Dynamic changes of the radiomics features over different phases may contain information of liver function. The relationship between these "delta parameters" and the liver function seems fascinating to explore.

As radiomics and machine learning has shown a powerful efficiency in the medical field, a radiomics model based on preoperative gadoxetic acid enhanced MRI for prediction of liver growth might supply more information to the surgeons. This could help them when planning portal vein embolization and liver resection.

A holistic software should be developed to take full advantage of the preoperative gadoxetic acid enhanced MRI. That is, to extract radiomics features from the normal hepatic tissue for liver function evaluation, PHLF prediction and liver growth estimation and to mine imaging features from the tumor region for biological behavior prediction, pathological grading estimation and microvascular invasion identification – in a word, to squeeze any possible information out of every single voxel on the gadoxetic acid enhanced MRI!

9 POPULAR SCIENCE SUMMARY OF THE THESIS

Liver cancer is one of the most common cancers in the world and liver resection is the mainstay in treatment of liver cancer with curative intent. To allow a safe liver resection, the future liver remnant, i.e. the remaining part after removal of the diseased liver must be sufficient, not only in volume but also function. In case that the remaining liver is insufficient after liver resection, deadly complications will occur, such as post-hepatectomy liver failure, for which no effective treatments are available except for supportive care or liver transplantation. Once occurred, the mortality of insufficient liver after resection can be as high as 80%.

It is therefore vital to thoroughly assess liver function preoperatively. Today this is done using blood tests or biochemical tests. The most common biochemical test is the ICG-15 test where a substance, indocyanine green, eliminated by the liver is injected and then quantified after 15 minutes. Unfortunately, these tests only provide liver function information on the whole liver, not taking the uneven distribution of liver function into account.

Currently, surgeons often make operation decision according to computed tomography based liver volumetry: the minimum remaining liver volume for a safe liver resection is 25-30% for a normal liver, while at least 40% for liver with cirrhosis or steatosis. However, volume is just a surrogate for liver function evaluation but volume is not always consistent with function. Due to chronic, repeatable tissue injury-repair processes different parts of the liver can be affected unevenly. This is more common in liver cancer patients, as they are often accompanied with chronic liver disease or have undergone previous chemotherapy. An approach which can evaluate regional liver function is warranted.

Gadoxetic acid is an MRI contrast agent which can make the normal tissue appear brighter while the diseased part appears darker, contributing to an excellent tissue contrast. Gadoxetic acid enhanced MRI is a widely used imaging technique for detecting and characterizing liver tumors. It is a liver specific contrast agent, taken up by the hepatic cells (“hepatocytes”) exclusively, in contrast with most other contrast agents which just stay in the vascular space. Researchers have found that with the severity of liver disease increasing, the absorption ability of the hepatocytes decreases. It means gadoxetic acid enhanced MRI can be applied to quantify liver function according to the degrees of imaging brightness.

Up to date, a plenty of gadoxetic acid enhanced MRI derived parameters have been proposed to estimate liver function based on different rationales. They can be roughly grouped into three categories: signal intensity (SI) based (how bright a tissue appears on the image), T1 relaxation time based (how fast the signal disappears) and dynamic hepatic contrast enhanced MRI based

parameters (based on more complex mathematical analyses of a serial of images). In **Study I**, we evaluated these three types of parameters and found that simple SI based parameters had a similar efficacy as the complex ones in assessment of liver function. Besides, the results revealed that liver-to-muscle ratio (LMR, calculated by SI of the liver divided by that of the muscle) had a good performance in discrimination of impaired liver function from the normal, in correlation with traditional scores for estimating liver function (the Child-Pugh score and Model for End-stage Liver Disease score).

In **Study II**, we evaluated the liver function and volume changes from preoperative baseline to postoperative day 7 and 28 in patients with colorectal liver metastases using MRI, ICG-R15 and hepatobiliary scintigraphy (a nuclear medicine imaging method). The findings showed that 1) LMR and hepatic uptake index (another SI-based parameter) had a good performance in assessment of liver function and prediction of remaining liver growth; 2) there were significant correlations between SI-based parameters and ICG-R15, and between SI-based parameters and hepatobiliary scintigraphy; 3) liver function had a similar alteration as the liver volume after liver resection within one month after liver resection.

Systematic review is a special review which collects all possible empirical literature according to a clearly formulated clinical question and draw an overall conclusion after critically appraisal the original studies, therefore it is regarded as the highest level of evidence. We performed a systematic review (**Study III**) to summarize currently available studies to evaluate the overall performance of gadoxetic acid enhanced MRI in prediction of post-operative liver failure. There were 15 eligible studies included in our research and the results showed that gadoxetic acid enhanced MRI had a high predictive accuracy in estimating the risk of liver failure after liver resection.

Radiomics is a branch of machine learning. It can extract a large number of features from clinically daily used medical images which usually cannot be detected by human naked eyes. The high dimension data can be mined for modelling via mathematical algorithm for diagnosis or prognostication of various diseases. In **Study IV**, we applied the radiomics approach on preoperative gadoxetic acid enhanced MRI for predicting liver failure in 276 patients with hepatocellular carcinoma who underwent liver resection. Our radiomics model showed an excellent discriminative ability in estimating the risk of post-hepatectomy liver failure in both training and test cohorts.

In conclusion, gadoxetic acid enhanced MRI seems to be a reliable and accurate tool for evaluation of liver function and prediction of liver failure.

10 ACKNOWLEDGEMENTS

How time flies! Having gone through the occasions of reading my peers' acknowledgements in their thesis, I have finally arrived at my turn. Looking back at this four-year study for my doctorate, I see a number of people who had helped, supported and accompanied me on this journey. Without them this end would not have materialized and hence I take this opportunity to express my gratitude to them. They made this long and tough journey a colorful and memorable one.

Prof. **Torkel Brismar**, my principal supervisor. Thank you for providing me with such a valuable opportunity to study at this world-class university. I came here with a rusty English skill and limited knowledge about MRI research, but you showed sufficient patience and gave me a flexible academic atmosphere which allowed me grow up gradually. You always liked to listen to my various ideas, guiding me to the correct direction in a subtle way. Thank you for the detailed, never-ending comments you made in the manuscript which reflected not just the substantial effort you contributed to my training, but also aroused my curiosity for scientific research and promoted me to be an independent researcher. Moreover, you are not just my supervisor, but also a good friend in life. You were always willing to help me on practical issues, tend to remind me to keep a work-life balance. Your attitude towards life, your love for sporting and cycling also exerted an impact on me. You set an excellent example of a fantastic supervisor.

Associate Prof. **Ernesto Sparrelid**, my co-supervisor. Your working style left me a lasting impression, quick, smart and sharp, just like your profession. This can be exemplified by your review on my papers, always hitting the core points, supplying insightful comments and getting back promptly. Thank you for your consistent instruction and guidance.

Prof. **Moustapha Hassan**, my co-supervisor. You are my wonderful, approachable and knowledgeable "boss", like pulling my leg to check I was still alive in the midst of my struggles and seeing me tearing my hair out. Thank you for your instructions on how to make a presentation. Thank you for your kind help and to know your office door was always open was most comforting. Thank you for the yearly lively barbeque at your home which already became a symbol of the Swedish summer for me. You are my dearest "boss" all the time.

Associate Prof. **Greg Nowak**, my co-supervisor (2018-2021). Although we did not meet frequently, I can still feel your passion for research through our limited talks. Thank you for sharing with me your fascinating ideas. I look forward to the future collaboration!

Prof. **Kuansheng Ma**, my master supervisor. Thank you for your consistent supervision and generous help from the very beginning of my master study to the end of my doctoral study. You are such a knowledgeable and farsighted instructor from whom I can always obtain inspirations whenever we talked. I am also grateful to Prof. **Lingfeng Zhu.** Thank you for your constant encouragement and care.

Senior researcher **Ying Zhao**. I amiably call you "Sister Ying" as you are so caring and warm-hearted, always happy to supply any help when needed. When you got off and passed by my office, you tended to give me a warm greeting, which made me feel you are always there for me. Thank you for your backup and support.

Dr. **Wenyi Zheng** and Chairman **Rui He,** Moutapha's fantastic couple students. I do not think common words can express my deepest gratitude to you, as the help and support on both academic and life aspects were countless. Special thanks also goes to the delicious, mouth-watering Sichuan cuisine at your home, which comforted my soul deeply through my stomach. Thank you for all of these.

A huge thanks to my ECM roommates (Moustapha's fantastic current and previous group members): Dr. **Sandra Oerther**, Dr. **Xiaoli Li** (and your son **Duoduo**), **Yikai Yin**, **Manon Renault**, **Zienab Mohammad**, docent **Manuchehr Abedi-Valugerdi**, Dr. **Ibrahim El-Serafi**, Dr. **Fadwa Benkessou**, Dr. **Risul Amin,** Dr. **Stefan Grudén** and Dr. **Fangyi Long** (and your wife Dr. **Ting Wang**). You are a group of friendly and brilliant guys, easy to get along and collaborate. Thank you for your generous help and every inspiring talk. The group activities we spent together were so impressive that I treasure them forever.

Many thanks to **Chengming Qu**, **Changfeng Li**, **Xiaojun Hu** and Prof. **Yingfang Fan**. Thank you for your support and trust. I learned a lot through the discussion about our projects. Look forward to our further collaborations!

I would like to thank **Savas Kessen** for showing me how to calculate various MRI parameters and introduced me into the MRI research. **Taha Berk Durukan** and **Kristoffer Sola**, thanks

for the kind talk and heated discussion during our mini-Journal Club. Thanks also goes to **Linn Berg** for kind help and support whenever I needed.

Dr. **Jiaxing Zhang**, thank you for guiding me to conduct a standard and rigorous systematic review/meta-analysis. Your extraordinary statistical knowledge, insight on methodologic research and open-mindedness left me with a deep impression. Thank you for your immediate and professional response whenever I bothered you.

Dr. **Yi Chen**, my first friend at KI. You are such a kind-hearted, generous, considerable (+100 positive adjectives) buddy. Your kind help started even before I came here, and it lasted through my whole PhD study period. Your enthusiasm for medical science, proficiency in bioinformatics, full energy for life and devotion to friends impressed me deeply, setting up a role model for me. Thank you for introducing me to so many fantastic places and wonderful food in Sweden. I believe you will realize your dream soon and a rosy future is waiting for you not far away.

Deepest gratitude also goes to: Dr. **Zheyu Niu** (and your wife **Xia Wang** and your son **Yuanda Niu**), Dr. **Xiuming Liang** and Dr. **Qing Wang** (and your twin girls, **Domy** and **Amy**), **Guannan Zhou**, **Xinyuan Liu**, Dr. **Xuan Li**, Dr. **Yulong Cai**, **Ye Yuan**, Prof. **Shuijie Li**, Dr. **Long Jiang** and **Feifei Yan,** Dr. **Xiaofang Cao**, **Yanhong Su**, Dr. **Leming Jia,** Dr. **Longkai Li**. Thank you for your warm company and the valuable friendship. The time with you guys was always lighthearted and enjoyable.

I would like to thank **China Scholarship Council (CSC)** for financing me to study abroad.

Special thanks to Dr. **Cecilia Aulin** and Prof. **Helena E. Harris** and the program of National Clinical Research School in Chronic Inflammatory Diseases (**NCRSCID**). Thank you for approving me as a member. Thank you for the well-organized events which not only broadened my academic vision but also got me meet so many eminent minds and intelligent, energetic young souls. I will be always proud as a member of the NCRSCID program.

I wish to acknowledge my thanks to the division administrators Dr. **Kathrin Reiser** and **Manuchehr Abedi-Valugerdi.** Thank you for your great effort in maintaining such a neat, tidy and cosy working environment for us.

Kind regards to my friends: **Anrong Wang** &**Juan Wang** (and your daughters **Yaya** and **Molly**), **Wei Zheng** &**Lei Tian** (and your son **Tian Zheng)**, **Mengxiao Zhu** &**Wei Tan (**and your daughter and son), **Yige Huang**, **May Lei Timms** (**Xu Meili**), **Zheng Li,** Dr. **Keyang Xu**, Prof. **Ling Zhou**, Dr. **Yu Zhang**, Dr. **Qing Cai**, Dr. **Bin Zhang**, **Xiu Zhao**, **Bo Zhao**. Thank you for your consistent support and company.

I would like to express my thanks to many cyber friends. Dr. **Renyuan Li,** thank you very much for your newbie-friendly and well-organized online teaching videos, which introduced me into the "Radiomics World". Dr. **Jianming Zeng** (**Jimmy**) and your team, "biotrainee", thank you for your huge piles of *R* language tutorials, which benefited me a lot in my research.

I would give my full gratitude and love to **Zhen Zheng**, my newly wedded wife. Thank you for accompanying me for such a long period in such a specific way: via video call at least one hour every day for the past three years (a really "virtual love"!). Thank you for the little doses of happiness you provided in my daily plain life. Thank you for cheering me up when my papers were repeatedly rejected and reminding me to pursue next when I achieved one goal. Thank you for backing me up always. Importantly, thank you for accepting imperfect me and tolerating my bad temper to be my wife.

To my family:

感谢母亲的养育之恩、无私宽厚的爱。谁言寸草心，报得三春晖！

感谢姐姐、姐夫，弟弟、弟妹，是你们的关心、支持，给了我底气和勇气在外面闯荡。感谢纯真的小朋友陈怡禾、王鸿铭、陈思源的陪伴。

感谢姑父、姑姑，表哥、表姐，以及你们温暖、和睦的大家庭。感谢你们对我的教育、培养，理解、支持。祝愿你们健康、平安、长寿。

感谢岳父母、舅舅、舅妈、外公、外婆、小朋友黄殊同、邱一诺，以及你们欢乐、有爱的大家庭。感谢你们的认可和信任，并且很荣幸成为这个大家庭的一员。

最后，把我最深切的思念和全部的荣耀都留给我的父亲。

11 REFERENCES

1. Ananthakrishnan A, Gogineni V, Saeian K. Epidemiology of primary and secondary liver cancers. Semin Intervent Radiol. 2006;23(1):47-63.

2. Forner A, Reig M, Bruix J. Hepatocellular carcinoma. The Lancet. 2018;391(10127):1301-1314.

3. Villanueva A. Hepatocellular Carcinoma. N Engl J Med. 2019;380(15):1450-1462.

4. Sayiner M, Golabi P, Younossi ZM. Disease Burden of Hepatocellular Carcinoma: A Global Perspective. Dig Dis Sci. 2019;64(4):910-917.

5. Grandhi MS, Kim AK, Ronnekleiv-Kelly SM, Kamel IR, Ghasebeh MA, Pawlik TM. Hepatocellular carcinoma: From diagnosis to treatment. SURG ONCOL. 2016;25(2):74-85.

6. Ye Q, Ling S, Zheng S, Xu X. Liquid biopsy in hepatocellular carcinoma: circulating tumor cells and circulating tumor DNA. MOL CANCER. 2019;18(1):114.

7. Dekker E, Tanis PJ, Vleugels JLA, Kasi PM, Wallace MB. Colorectal cancer. The Lancet. 2019;394(10207):1467-1480.

8. Linecker M, Kuemmerli C, Clavien PA, Petrowsky H. Dealing with insufficient liver remnant: Associating liver partition and portal vein ligation for staged hepatectomy. J SURG ONCOL. 2019;119(5):604-612.

9. Bruix J, Sherman M. Management of hepatocellular carcinoma. HEPATOLOGY. 2005;42(5):1208-1236.

10. Jarnagin WR, Gonen M, Fong Y, DeMatteo RP, Ben-Porat L, Little S, et al. Improvement in perioperative outcome after hepatic resection: analysis of 1,803 consecutive cases over the past decade. ANN SURG. 2002;236(4):397-406; discussion 406-397.

11. Tustumi F, Ernani L, Coelho FF, Bernardo WM, Junior SS, Kruger JAP, et al. Preoperative strategies to improve resectability for hepatocellular carcinoma: a systematic review and meta-analysis. HPB (Oxford). 2018;20(12):1109-1118.

12. Pawlik TM, Schulick RD, Choti MA. Expanding criteria for resectability of colorectal liver metastases. Oncologist. 2008;13(1):51-64.

13. Wang Q, Yan J, Feng X, Chen G, Xia F, Li X, et al. Safety and efficacy of radiofrequency-assisted ALPPS (RALPPS) in patients with cirrhosis-related hepatocellular carcinoma. Int J Hyperthermia. 2017;33(7):846-852.

14. Pandanaboyana S, Bell R, Hidalgo E, Toogood G, Prasad KR, Bartlett A, et al. A systematic review and meta-analysis of portal vein ligation versus portal vein embolization for elective liver resection. SURGERY. 2015;157(4):690-698.

15. Ali A, Ahle M, Bjornsson B, Sandstrom P. Portal vein embolization with N-butyl cyanoacrylate glue is superior to other materials: a systematic review and meta-analysis. EUR RADIOL. 2021.

16. Kim D, Cornman-Homonoff J, Madoff DC. Preparing for liver surgery with "Alphabet Soup": PVE, ALPPS, TAE-PVE, LVD and RL. Hepatobiliary Surg Nutr. 2020;9(2):136-151.

17. de Santibanes E, Clavien PA. Playing Play-Doh to prevent postoperative liver failure: the "ALPPS" approach. ANN SURG. 2012;255(3):415-417.

18. Schnitzbauer AA, Lang SA, Goessmann H, Nadalin S, Baumgart J, Farkas SA, et al. Right portal vein ligation combined with in situ splitting induces rapid left lateral liver lobe hypertrophy enabling 2-staged extended right hepatic resection in small-for-size settings. ANN SURG. 2012;255(3):405-414.

19. Lang H, Baumgart J. Associated Liver Partition and Portal Vein Ligation for Staged Hepatectomy (ALPPS) Registry: What Have We Learned? 2020.

20. Garcea G, Maddern GJ. Liver failure after major hepatic resection. J Hepatobiliary Pancreat Surg. 2009;16(2):145-155.

21. Ferrero A, Viganò L, Polastri R, Muratore A, Eminefendic H, Regge D, et al. Postoperative liver dysfunction and future remnant liver: where is the limit? Results of a prospective study. WORLD J SURG. 2007;31(8):1643-1651.

22. Ba-Ssalamah A, Bastati N, Wibmer A, Fragner R, Hodge JC, Trauner M, et al. Hepatic gadoxetic acid uptake as a measure of diffuse liver disease: Where are we? J MAGN RESON IMAGING. 2017;45(3):646-659.

23. Cieslak KP, Runge JH, Heger M, Stoker J, Bennink RJ, van Gulik TM. New Perspectives in the Assessment of Future Remnant Liver. DIGEST SURG. 2014;31(4-5):255-268.

24. Johnson PJ, Berhane S, Kagebayashi C, Satomura S, Teng M, Reeves HL, et al. Assessment of liver function in patients with hepatocellular carcinoma: a new evidence-based approach-the ALBI grade. J CLIN ONCOL. 2015;33(6):550-558.

25. Hiraoka A, Kumada T, Kudo M, Hirooka M, Tsuji K, Itobayashi E, et al. Albumin-Bilirubin (ALBI) Grade as Part of the Evidence-Based Clinical Practice Guideline for HCC of the Japan Society of Hepatology: A Comparison with the Liver Damage and Child-Pugh Classifications. LIVER CANCER. 2017;6(3):204-215.

26. Reig M, Forner A, Rimola J, Ferrer-Fabrega J, Burrel M, Garcia-Criado A, et al. BCLC strategy for prognosis prediction and treatment recommendation: The 2022 update. J HEPATOL. 2022;76(3):681-693.

27. Na SK, Yim SY, Suh SJ, Jung YK. ALBI versus Child-Pugh grading systems for liver function in patients with hepatocellular carcinoma. J SURG ONCOL. 2018;117(5):912-921.

28. Lee HJ, Hong SB, Lee NK, Kim S, Seo HI, Kim DU, et al. Validation of functional liver imaging scores (FLIS) derived from gadoxetic acid-enhanced MRI in patients with chronic liver disease and liver cirrhosis: the relationship between Child-Pugh score and FLIS. EUR RADIOL. 2021;31(11):8606-8614.

29. Kamath PS, Wiesner RH, Malinchoc M, Kremers W, Therneau TM, Kosberg CL, et al. A model to predict survival in patients with end-stage liver disease. HEPATOLOGY. 2001;33(2):464-470.

30. Nagashima I, Takada T, Okinaga K, Nagawa H. A scoring system for the assessment of the risk of mortality after partial hepatectomy in patients with chronic liver dysfunction. J Hepatobiliary Pancreat Surg. 2005;12(1):44-48.

31. Vos JJ, Wietasch JKG, Absalom AR, Hendriks HGD, Scheeren TWL. Green light for liver function monitoring using indocyanine green? An overview of current clinical applications. ANAESTHESIA. 2014;69(12):1364-1376.

32. Shen YN, Zheng ML, Guo CX, Bai XL, Pan Y, Yao WY, et al. The role of imaging in prediction of post-hepatectomy liver failure. CLIN IMAG. 2018;52:137-145.

33. Clavien PA, Petrowsky H, DeOliveira ML, Graf R. Strategies for safer liver surgery and partial liver transplantation. N Engl J Med. 2007;356(15):1545-1559.

34. Nilsson H, Blomqvist L, Douglas L, Nordell A, Janczewska I, Naslund E, et al. Gd-EOB-DTPA-enhanced MRI for the assessment of liver function and volume in liver cirrhosis. Br J Radiol. 2013;86(1026):20120653.

35. Guglielmi A, Ruzzenente A, Conci S, Valdegamberi A, Iacono C. How much remnant is enough in liver resection? Dig Surg. 2012;29(1):6-17.

36. Du S, Mao Y, Tong J, Li F, Che L, Li S, et al. A novel liver function evaluation system using radiopharmacokinetic modeling of technetium-99m-DTPA-galactosyl human serum albumin. NUCL MED COMMUN. 2013;34(9):893-899.

37. Kishi Y, Abdalla EK, Chun YS, Zorzi D, Madoff DC, Wallace MJ, et al. Three hundred and one consecutive extended right hepatectomies: evaluation of outcome based on systematic liver volumetry. ANN SURG. 2009;250(4):540-548.

38. Nilsson H, Karlgren S, Blomqvist L, Jonas E. The inhomogeneous distribution of liver function: possible impact on the prediction of post-operative remnant liver function. HPB (Oxford). 2015;17(3):272-277.

39. Joo I, Lee JM. Recent Advances in the Imaging Diagnosis of Hepatocellular Carcinoma: Value of Gadoxetic Acid-Enhanced MRI. LIVER CANCER. 2016;5(1):67-87.

40. Van Beers BE, Pastor CM, Hussain HK. Primovist, Eovist: what to expect? J HEPATOL. 2012;57(2):421-429.

41. Choi Y, Huh J, Woo DC, Kim KW. Use of gadoxetate disodium for functional MRI based on its unique molecular mechanism. Br J Radiol. 2016;89(1058):20150666.

42. Brismar TB, Dahlstrom N, Edsborg N, Persson A, Smedby O, Albiin N. Liver vessel enhancement by Gd-BOPTA and Gd-EOB-DTPA: a comparison in healthy volunteers. ACTA RADIOL. 2009;50(7):709-715.

43. Ricke J, Seidensticker M. Molecular imaging and liver function assessment by hepatobiliary MRI. J HEPATOL. 2016;65(6):1081-1082.

44. Verloh N, Haimerl M, Zeman F, Schlabeck M, Barreiros A, Loss M, et al. Assessing liver function by liver enhancement during the hepatobiliary phase with Gd-EOB-DTPA-enhanced MRI at 3 Tesla. EUR RADIOL. 2014;24(5):1013-1019.

45. Bae KE, Kim SY, Lee SS, Kim KW, Won HJ, Shin YM, et al. Assessment of hepatic function with Gd-EOB-DTPA-enhanced hepatic MRI. Dig Dis. 2012;30(6):617-622.

46. Haimerl M, Verloh N, Zeman F, Fellner C, Nickel D, Lang SA, et al. Gd-EOB-DTPA-enhanced MRI for evaluation of liver function: Comparison between signal-intensity-based indices and T1 relaxometry. Sci Rep. 2017;7:43347.

47. Besa C, Bane O, Jajamovich G, Marchione J, Taouli B. 3D T1 relaxometry pre and post gadoxetic acid injection for the assessment of liver cirrhosis and liver function. MAGN RESON IMAGING. 2015;33(9):1075-1082.

48. Katsube T, Okada M, Kumano S, Hori M, Imaoka I, Ishii K, et al. Estimation of liver function using T1 mapping on Gd-EOB-DTPA-enhanced magnetic resonance imaging. INVEST RADIOL. 2011;46(4):277-283.

49. Ryeom HK, Kim SH, Kim JY, Kim HJ, Lee JM, Chang YM, et al. Quantitative evaluation of liver function with MRI Using Gd-EOB-DTPA. KOREAN J RADIOL. 2004;5(4):231-239.

50. Lagadec M, Doblas S, Giraudeau C, Ronot M, Lambert SA, Fasseu M, et al. Advanced fibrosis: Correlation between pharmacokinetic parameters at dynamic gadoxetate-enhanced MR imaging and hepatocyte organic anion transporter expression in rat liver. RADIOLOGY. 2015;274(2):379-386.

51. Sourbron S, Sommer WH, Reiser MF, Zech CJ. Combined quantification of liver perfusion and function with dynamic gadoxetic acid-enhanced MR imaging. RADIOLOGY. 2012;263(3):874-883.

52. Gillies RJ, Kinahan PE, Hricak H. Radiomics: Images Are More than Pictures, They Are Data. RADIOLOGY. 2016;278(2):563-577.

53. Lambin P, Leijenaar RTH, Deist TM, Peerlings J, de Jong EEC, van Timmeren J, et al. Radiomics: the bridge between medical imaging and personalized medicine. NAT REV CLIN ONCOL. 2017;14(12):749-762.

54. van Griethuysen JJM, Fedorov A, Parmar C, Hosny A, Aucoin N, Narayan V, et al. Computational Radiomics System to Decode the Radiographic Phenotype. CANCER RES. 2017;77(21):e104-e107.

55. Tomaszewski MR, Gillies RJ. The Biological Meaning of Radiomic Features. RADIOLOGY. 2021;298(3):505-516.

56. Wei J, Jiang H. Radiomics in liver diseases: Current progress and future opportunities. LIVER INT. 2020;40(9):2050-2063.

57. Miranda Magalhaes Santos JM, Clemente Oliveira B, Araujo-Filho JAB, Assuncao-Jr AN, de MMFA, Carlos Tavares Rocha C, et al. State-of-the-art in radiomics of hepatocellular carcinoma: a review of basic principles, applications, and limitations. Abdom Radiol (NY). 2020;45(2):342-353.

58. Shi Z, Cai W, Feng X, Cai J, Liang Y, Xu J, et al. Radiomics Analysis of Gd-EOB-DTPA Enhanced Hepatic MRI for Assessment of Functional Liver Reserve. ACAD RADIOL. 2022;29(2):213-218.

59. Wu J, Xie F, Ji H, Zhang Y, Luo Y, Xia L, et al. A Clinical-Radiomic Model for Predicting Indocyanine Green Retention Rate at 15 Min in Patients With Hepatocellular Carcinoma. FRONT SURG. 2022;9:857838.

60. Simpson AL, Adams LB, Allen PJ, D'Angelica MI, DeMatteo RP, Fong Y, et al. Texture analysis of preoperative CT images for prediction of postoperative hepatic insufficiency: a preliminary study. J Am Coll Surg. 2015;220(3):339-346.

61. Pan Z, Cai W, He B, Hu M, Zhang W, Xiao D, et al. A radiomics-based nomogram for the preoperative prediction of posthepatectomy liver failure in patients with hepatocellular carcinoma. ACTA RADIOL. 2019;28:78-85.

62. Chen Y, Liu Z, Mo Y, Li B, Zhou Q, Peng S, et al. Prediction of Post-hepatectomy Liver Failure in Patients With Hepatocellular Carcinoma Based on Radiomics

Using Gd-EOB-DTPA-Enhanced MRI: The Liver Failure Model. FRONT ONCOL. 2021;11:605296.

63. Zhu WS, Shi SY, Yang ZH, Song C, Shen J. Radiomics model based on preoperative gadoxetic acid-enhanced MRI for predicting liver failure. WORLD J GASTROENTERO. 2020;26(11):1208-1220.

64. Schreckenbach T, Liese J, Bechstein WO, Moench C. Posthepatectomy liver failure. Dig Surg. 2012;29(1):79-85.

65. van den Broek MA, Olde Damink SW, Dejong CH, Lang H, Malagó M, Jalan R, et al. Liver failure after partial hepatic resection: definition, pathophysiology, risk factors and treatment. LIVER INT. 2008;28(6):767-780.

66. Lafaro K, Buettner S, Maqsood H, Wagner D, Bagante F, Spolverato G, et al. Defining Post Hepatectomy Liver Insufficiency: Where do We stand? J GASTROINTEST SURG. 2015;19(11):2079-2092.

67. Wang Q, Wang A, Sparrelid E, Zhang J, Zhao Y, Ma K, et al. Predictive value of gadoxetic acid-enhanced MRI for posthepatectomy liver failure: a systematic review. EUR RADIOL. 2021.

68. Mehrabi A, Golriz M, Khajeh E, Ghamarnejad O, Probst P, Fonouni H, et al. Meta-analysis of the prognostic role of perioperative platelet count in posthepatectomy liver failure and mortality. Br J Surg. 2018;105(10):1254-1261.

69. Rassam F, Zhang T, Cieslak KP, Lavini C, Stoker J, Bennink RJ, et al. Comparison between dynamic gadoxetate-enhanced MRI and Tc-99m-mebrofenin hepatobiliary scintigraphy with SPECT for quantitative assessment of liver function. EUR RADIOL. 2019;29(9):5063-5072.

70. Laurent C, Sa Cunha A, Couderc P, Rullier E, Saric J. Influence of postoperative morbidity on long-term survival following liver resection for colorectal metastases. Br J Surg. 2003;90(9):1131-1136.

71. Rahbari NN, Garden OJ, Padbury R, Brooke-Smith M, Crawford M, Adam R, et al. Posthepatectomy liver failure: a definition and grading by the International Study Group of Liver Surgery (ISGLS). SURGERY. 2011;149(5):713-724.

72. Balzan S, Belghiti J, Farges O, Ogata S, Sauvanet A, Delefosse D, et al. The "50-50 criteria" on postoperative day 5: an accurate predictor of liver failure and death after hepatectomy. ANN SURG. 2005;242(6):824-828, discussion 828-829.

73. Kauffmann R, Fong Y. Post-hepatectomy liver failure. Hepatobiliary Surg Nutr. 2014;3(5):238-246.

74. Jin S, Fu Q, Wuyun G, Wuyun T. Management of post-hepatectomy complications. World J Gastroenterol. 2013;19(44):7983-7991.

75. Gilg S, Sparrelid E, Saraste L, Nowak G, Wahlin S, Stromberg C, et al. The molecular adsorbent recirculating system in posthepatectomy liver failure: Results from a prospective phase I study. HEPATOL COMMUN. 2018;2(4):445-454.

76. Sparrelid E, Gilg S, van Gulik TM. Systematic review of MARS treatment in post-hepatectomy liver failure. HPB (Oxford). 2020;22(7):950-960.

77. Chan SC, Sharr WW, Chan AC, Chok KS, Lo CM. Rescue Living-donor Liver Transplantation for Liver Failure Following Hepatectomy for Hepatocellular Carcinoma. LIVER CANCER. 2013;2(3-4):332-337.

78. Tamada T, Ito K, Higaki A, Yoshida K, Kanki A, Sato T, et al. Gd-EOB-DTPA-enhanced MR imaging: evaluation of hepatic enhancement effects in normal and cirrhotic livers. EUR J RADIOL. 2011;80(3):e311-316.

79. Kubota K, Tamura T, Aoyama N, Nogami M, Hamada N, Nishioka A, et al. Correlation of liver parenchymal gadolinium-ethoxybenzyl diethylenetriaminepentaacetic acid enhancement and liver function in humans with hepatocellular carcinoma. ONCOL LETT. 2012;3(5):990-994.

80. Kamimura K, Fukukura Y, Yoneyama T, Takumi K, Tateyama A, Umanodan A, et al. Quantitative evaluation of liver function with T1 relaxation time index on Gd-EOB-DTPA-enhanced MRI: comparison with signal intensity-based indices. J MAGN RESON IMAGING. 2014;40(4):884-889.

81. Dahlqvist Leinhard O, Dahlstrom N, Kihlberg J, Sandstrom P, Brismar TB, Smedby O, et al. Quantifying differences in hepatic uptake of the liver specific contrast agents Gd-EOB-DTPA and Gd-BOPTA: a pilot study. EUR RADIOL. 2012;22(3):642-653.

82. Nishie A, Ushijima Y, Tajima T, Asayama Y, Ishigami K, Kakihara D, et al. Quantitative analysis of liver function using superparamagnetic iron oxide- and Gd-EOB-DTPA-enhanced MRI: comparison with Technetium-99m galactosyl serum albumin scintigraphy. EUR J RADIOL. 2012;81(6):1100-1104.

83. Yamada A, Hara T, Li F, Fujinaga Y, Ueda K, Kadoya M, et al. Quantitative evaluation of liver function with use of gadoxetate disodium-enhanced MR imaging. RADIOLOGY. 2011;260(3):727-733.

84. de Bazelaire CM, Duhamel GD, Rofsky NM, Alsop DC. MR imaging relaxation times of abdominal and pelvic tissues measured in vivo at 3.0 T: preliminary results. RADIOLOGY. 2004;230(3):652-659.

85. Nilsson H, Nordell A, Vargas R, Douglas L, Jonas E, Blomqvist L. Assessment of hepatic extraction fraction and input relative blood flow using dynamic hepatocyte-specific contrast-enhanced MRI. J MAGN RESON IMAGING. 2009;29(6):1323-1331.

86. Ribero D, Chun YS, Vauthey JN. Standardized liver volumetry for portal vein embolization. Semin Intervent Radiol. 2008;25(2):104-109.

87. Sparrelid E, Jonas E, Tzortzakakis A, Dahlen U, Murquist G, Brismar T, et al. Dynamic Evaluation of Liver Volume and Function in Associating Liver Partition and Portal Vein Ligation for Staged Hepatectomy. J GASTROINTEST SURG. 2017;21(6):967-974.

88. Liberati A, Altman DG, Tetzlaff J, Mulrow C, Gøtzsche PC, Ioannidis JP, et al. The PRISMA statement for reporting systematic reviews and meta-analyses of studies that evaluate healthcare interventions: explanation and elaboration. Bmj. 2009;339:b2700.

89. Hayden JA, van der Windt DA, Cartwright JL, Côté P, Bombardier C. Assessing bias in studies of prognostic factors. ANN INTERN MED. 2013;158(4):280-286.

90. Dahiya D, Wu TJ, Lee CF, Chan KM, Lee WC, Chen MF. Minor versus major hepatic resection for small hepatocellular carcinoma (HCC) in cirrhotic patients: a 20-year experience. SURGERY. 2010;147(5):676-685.

91. Liang M, Zhao J, Xie B, Li C, Yin X, Cheng L, et al. MR liver imaging with Gd-EOB-DTPA: The need for different delay times of the hepatobiliary phase in patients with different liver function. EUR J RADIOL. 2016;85(3):546-552.

92. Zwanenburg A, Vallières M. The Image Biomarker Standardization Initiative: Standardized Quantitative Radiomics for High-Throughput Image-based Phenotyping. 2020;295(2):328-338.

93. Koo TK, Li MY. A Guideline of Selecting and Reporting Intraclass Correlation Coefficients for Reliability Research. J Chiropr Med. 2016;15(2):155-163.

94. Gu D, Xie Y, Wei J, Li W, Ye Z, Zhu Z, et al. MRI-Based Radiomics Signature: A Potential Biomarker for Identifying Glypican 3-Positive Hepatocellular Carcinoma. J MAGN RESON IMAGING. 2020;52(6):1679-1687.

95. Vrieze SI. Model selection and psychological theory: a discussion of the differences between the Akaike information criterion (AIC) and the Bayesian information criterion (BIC). PSYCHOL METHODS. 2012;17(2):228-243.

96. Steyerberg EW, Vickers AJ, Cook NR, Gerds T, Gonen M, Obuchowski N, et al. Assessing the performance of prediction models: a framework for traditional and novel measures. EPIDEMIOLOGY. 2010;21(1):128-138.

97. Vickers AJ, van Calster B, Steyerberg EW. A simple, step-by-step guide to interpreting decision curve analysis. Diagn Progn Res. 2019;3:18.

98. Cho SH, Kang UR, Kim JD, Han YS, Choi DL. The value of gadoxetate disodium-enhanced MR imaging for predicting posthepatectomy liver failure after major hepatic resection: a preliminary study. EUR J RADIOL. 2011;80(2):e195-200.

99. Wibmer A, Prusa AM, Nolz R, Gruenberger T, Schindl M, Ba-Ssalamah A. Liver failure after major liver resection: risk assessment by using preoperative Gadoxetic acid-enhanced 3-T MR imaging. RADIOLOGY. 2013;269(3):777-786.

100. Sato Y, Matsushima S, Inaba Y, Sano T, Yannaura H, Kato M, et al. Preoperative Estimation of Future Remnant Liver Function Following Portal Vein Embolization Using Relative Enhancement on Gadoxetic Acid Disodium-Enhanced Magnetic Resonance Imaging. KOREAN J RADIOL. 2015;16(3):523-530.

101. Jin YJ, Lee SH, Cho SG, Kim JH, Lee JW, Lee KY, et al. Prediction of postoperative liver failure using gadoxetic acid-enhanced magnetic resonance imaging in patients with hepatocellular carcinoma. J Gastroenterol Hepatol. 2016;31(7):1349-1356.

102. Costa AF, Tremblay St-Germain A, Abdolell M, Smoot RL, Cleary S, Jhaveri KS. Can contrast-enhanced MRI with gadoxetic acid predict liver failure and other complications after major hepatic resection? CLIN RADIOL. 2017;72(7):598-605.

103. Asenbaum U, Kaczirek K, Ba-Ssalamah A, Ringl H, Schwarz C, Waneck F, et al. Post-hepatectomy liver failure after major hepatic surgery: not only size matters. 2018;28(11):4748-4756.

104. Chuang YH, Ou HY, Lazo MZ, Chen CL, Chen MH, Weng CC, et al. Predicting post-hepatectomy liver failure by combined volumetric, functional MR image and laboratory analysis. LIVER INT. 2018;38(5):868-874.

105. Kim DK, Choi JI, Choi MH, Park MY, Lee YJ, Rha SE, et al. Prediction of Posthepatectomy Liver Failure: MRI With Hepatocyte-Specific Contrast Agent Versus Indocyanine Green Clearance Test. AJR Am J Roentgenol. 2018;211(3):580-587.

106. Theilig D, Steffen I, Malinowski M, Stockmann M, Seehofer D, Pratschke J, et al. Predicting liver failure after extended right hepatectomy following right portal vein embolization with gadoxetic acid-enhanced MRI. EUR RADIOL. 2019;29(11):5861-5872.

107. Araki K, Harimoto N, Kubo N, Watanabe A, Igarashi T, Tsukagoshi M, et al. Functional remnant liver volumetry using Gd-EOB-DTPA-enhanced magnetic resonance imaging (MRI) predicts post-hepatectomy liver failure in resection of more than one segment. HPB (Oxford). 2020;22(2):318-327.

108. Donadon M, Lanza E, Branciforte B, Muglia R, Lisi C, Pedicini V, et al. Hepatic uptake index in the hepatobiliary phase of gadolinium ethoxybenzyl diethylenetriamine penta acetic acid-enhanced magnetic resonance imaging estimates functional liver reserve and predicts post-hepatectomy liver failure. SURGERY. 2020;168(3):419-425.

109. Orimo T, Kamiyama T, Kamachi H, Shimada S, Nagatsu A, Asahi Y, et al. Predictive value of gadoxetic acid enhanced magnetic resonance imaging for posthepatectomy liver failure after a major hepatectomy. J Hepatobiliary Pancreat Sci. 2020;27(8):531-540.

110. Zhu WS, Shi SY, Yang ZH, Song C, Shen J. Radiomics model based on preoperative gadoxetic acid-enhanced MRI for predicting liver failure. World J Gastroenterol. 2020;26(11):1208-1220.

111. Tsujita Y, Sofue K, Komatsu S, Yamaguchi T, Ueshima E, Ueno Y, et al. Prediction of post-hepatectomy liver failure using gadoxetic acid-enhanced magnetic resonance imaging for hepatocellular carcinoma with portal vein invasion. EUR J RADIOL. 2020;130:109189.

112. Wang Y, Zhang L, Ning J, Zhang X, Li X, Zhang L, et al. Preoperative Remnant Liver Function Evaluation Using a Routine Clinical Dynamic Gd-EOB-DTPA-Enhanced MRI Protocol in Patients with Hepatocellular Carcinoma. ANN SURG ONCOL. 2020.

113. Kim J-E, Kim JH, Park SJ, Choi S-Y, Yi N-J, Han JK. Prediction of liver remnant regeneration after living donor liver transplantation using preoperative CT texture analysis. ABDOM RADIOL. 2019;44(5):1785-1794.

114. Moris D, Vernadakis S, Papalampros A, Vailas M, Dimitrokallis N, Petrou A, et al. Mechanistic insights of rapid liver regeneration after associating liver partition and portal vein ligation for stage hepatectomy. World J Gastroenterol. 2016;22(33):7613-7624.

115. Leung U, Simpson AL, Araujo RL, Gonen M, McAuliffe C, Miga MI, et al. Remnant growth rate after portal vein embolization is a good early predictor of post-hepatectomy liver failure. J Am Coll Surg. 2014;219(4):620-630.

116. Barth BK, Fischer MA, Kambakamba P, Lesurtel M, Reiner CS. Liver-fat and liver-function indices derived from Gd-EOB-DTPA-enhanced liver MRI for prediction of future liver remnant growth after portal vein occlusion. EUR J RADIOL. 2016;85(4):843-849.

117. Hindel S, Geisel D, Aleric I, Theilig D, Denecke T, Ludemann L. Liver function quantification of patients with portal vein embolization using dynamic contrast-enhanced MRI for assessment of hepatocyte uptake and elimination. Phys Med. 2020;76:207-220.

118. Geisel D, Raabe P, Ludemann L, Malinowski M, Stockmann M, Seehofer D, et al. Gd-EOB-DTPA-enhanced MRI for monitoring future liver remnant function after portal vein embolization and extended hemihepatectomy: A prospective trial. EUR RADIOL. 2017;27(7):3080-3087.

119. Heil J, Heid F, Bechstein WO, Bjornsson B, Brismar TB, Carling U, et al. Sarcopenia predicts reduced liver growth and reduced resectability in patients undergoing portal vein embolization before liver resection - A DRAGON collaborative analysis of 306 patients. HPB (Oxford). 2022;24(3):413-421.

120. Heil J, Korenblik R, Heid F, Bechstein WO, Bemelmans M, Binkert C, et al. Preoperative portal vein or portal and hepatic vein embolization: DRAGON collaborative group analysis. Br J Surg. 2021;108(7):834-842.

121. Shindoh J, Tzeng CW, Aloia TA, Curley SA, Huang SY, Mahvash A, et al. Safety and efficacy of portal vein embolization before planned major or extended hepatectomy: an institutional experience of 358 patients. J GASTROINTEST SURG. 2014;18(1):45-51.

122. Gong W-F, Zhong J-H, Lu Z, Zhang Q-M, Zhang Z-Y, Chen C-Z, et al. Evaluation of liver regeneration and post-hepatectomy liver failure after hemihepatectomy in patients with hepatocellular carcinoma. BIOSCIENCE REP. 2019;39(8).

123. Kang HJ, Ahn SJ, Yang H, Kim E, Okuaki T, Han JK, et al. Gd-EOB-DTPA-enhanced MRI T1 mapping for assessment of liver function in rabbit fibrosis model: comparison of hepatobiliary phase images obtained at 10 and 20 min. RADIOLOGY. 2017;122(4):239-247.

124. Ding Y, Rao SX, Zhu T, Chen CZ, Li RC, Zeng MS. Liver fibrosis staging using T1 mapping on gadoxetic acid-enhanced MRI compared with DW imaging. CLIN RADIOL. 2015;70(10):1096-1103.

125. Nakagawa M, Namimoto T, Shimizu K, Morita K, Sakamoto F, Oda S, et al. Measuring hepatic functional reserve using T1 mapping of Gd-EOB-DTPA enhanced 3T MR imaging: A preliminary study comparing with (99m)Tc GSA scintigraphy and signal intensity based parameters. EUR J RADIOL. 2017;92:116-123.

126. Yoon JH, Lee JM, Kang HJ, Ahn SJ, Yang H, Kim E, et al. Quantitative Assessment of Liver Function by Using Gadoxetic Acid-enhanced MRI: Hepatocyte Uptake Ratio. RADIOLOGY. 2019;290(1):125-133.

127. Møller S, la Cour Sibbesen E, Madsen JL, Bendtsen F. Indocyanine green retention test in cirrhosis and portal hypertension: Accuracy and relation to severity of disease. J Gastroenterol Hepatol. 2019;34(6):1093-1099.

128. Wakiya T, Kudo D, Toyoki Y, Ishido K, Kimura N, Narumi S, et al. Evaluation of the usefulness of the indocyanine green clearance test for chemotherapy-associated liver injury in patients with colorectal cancer liver metastasis. ANN SURG ONCOL. 2014;21(1):167-172.

129. Hiraoka A, Kumada T, Michitaka K, Kudo M. Newly Proposed ALBI Grade and ALBI-T Score as Tools for Assessment of Hepatic Function and Prognosis in Hepatocellular Carcinoma Patients. LIVER CANCER. 2019;8(5):312-325.

130. Xiang F, Liang X, Yang L, Liu X, Yan S. CT radiomics nomogram for the preoperative prediction of severe post-hepatectomy liver failure in patients with huge (>/= 10 cm) hepatocellular carcinoma. WORLD J SURG ONCOL. 2021;19(1):344.

131. Fan M, Chen H, You C, Liu L, Gu Y, Peng W, et al. Radiomics of Tumor Heterogeneity in Longitudinal Dynamic Contrast-Enhanced Magnetic Resonance Imaging for Predicting Response to Neoadjuvant Chemotherapy in Breast Cancer. FRONT MOL BIOSCI. 2021;8:622219.